SOLID-STATE CHARACTERIZATION AND ENGINEERING OF TWO ANTIHISTAMINE DRUGS - LORATADINE AND DESLORATADINE

A THESIS
SUBMITTED TO THE FACULTY OF
UNIVERSITY OF MINNESOTA
BY

Zhongyang Shi

IN PARTIAL FULFILLMENT OF THE REQUIREMENTS
FOR THE DEGREE OF
MASTER OF SCIENCE

Changquan Calvin Sun, Advisor

June, 2019

Acknowledgements

My two-year journey of graduate study as a master student seems like only yesterday. Many people gave their hands to me and made this journey full of kindness and gain. I would like to begin with my appreciation to my advisor, Dr. Changquan Calvin Sun, for his guidance and help. As a professor, he is very knowledgeable and has his own professional insight into nearly every single field within solid state pharmaceuticals. As a mentor, he is willing to spare time talking with me and taught me not only how to solve my research problems but also the right attitudes and habits to conduct research. His constructive comments inspired me a lot and helped me became more organized and thoughtful when facing a project, which would be a great treasure for me in my future career.

My days in the Sun laboratory have been enjoyable as well. I would like to thank the postdocs, Dr. Chenguang Wang, Dr. Shubhajit Paul and Dr. Manish Mishra, for their guidance from their practical experience. They are all expert scientists in their fields. I especially thank Dr. Chenguang Wang for being my project collaborator and manuscript coauthor. He helped polish my project and gave a lot of useful feedbacks. My thanks also go to Wei-Jhe, Shao-Yu, Jiangnan, Shenye, Kunlin, Hongbo, Yiwang and Ling for their company. They are all good examples of senior students in a lab. They gave me training

on instruments, correcting my mistakes in experiments and gave me tips on how to survive in a strange city.

I am grateful to Drs. Timothy S. Wiedmann and Nathan Mara for being on my thesis committee. Dr. Wiedmann is always ready to help students and I especially thank him for critical review of my application materials.

I thank my classmates, Xueyao, Lushan, Rachel, Jiawei, Sibo and Jayesh, for their company. Our similar course schedule and research life gave us shared feelings. To have them as listeners of my experience relieved my stress a lot.

Finally, I would like to thank my parents. Thank you for supporting my decision to study abroad. Your financial support made sure I can concentrate on study and live a healthy life. Your mental support made me feel less homesick and always raised me up when I was trapped by problems of all kinds. I cannot achieve my goals without you looking from behind.

Dedication

To my family

Abstract

With the implementation of Quality by Design (QbD), pharmaceutical product development is gradually transforming from an art based on empirical practice to a science based on knowledge of material and process. In this thesis work, we employed two classic antihistamine drugs – loratadine (Lor) and desloratadine (Des) as model compounds. The more superior tabletability of Lor than that of Des is explained by the bonding area (BA) and bonding strength (BS) model. The molecular origins of both BA and BS are systematically investigated, which can be applied to effectively improve mechanical properties and tableting performance of drugs. The problems of poor water solubility and dissolution rate of Lor at physiological pHs is overcome through crystal engineering that leads to a new multicomponent crystalline form of Lor with an artificial sweetener, saccharin. The sweet taste, enhanced solubility and dissolution rate, as well as acceptable physical stability of the new salt facilitate the development of a chewable tablet formulation, demonstrating the usefulness of crystal engineering in pharmaceutical development of chewable tablets. New insights into the relationship between crystal structure and macroscopic bulk powder compaction behavior were gained from this research.

Table of contents

List of Tables

List of Figures

CHAPTER 1 Introduction

1.1 General Introduction

The goal of pharmaceutical science is to develop safe, effective and economical drug products for the well-being of the general public. For a typical solid dosage form of small molecule drugs, the discovery of a New Chemical Entity is just the beginning of a long journey full of challenges. A chemical compound must go through several key steps before it can be produced as a drug product for clinical trials. First, the solid-state screening is conducted to determine the most appropriate solid form, including polymorphs, salts and cocrystals, for development.[1] Solubility, bioavailability, powder flow, compression, thermal stability, hygroscopicity, and a number of other properties are all taken into consideration to render a solid form with best performance. Once the proper solid form of the compound is selected, formulation development is followed to further modify the properties and overcome the drawbacks of the drug with the aid of excipients. The stability, safety, efficacy, manufacturability, and patient compliance are expected to be improved with a judiciously designed formulation.[2] Finally, all manufacturing processes involved to produce the drug product need to be assessed. For example, for a direct compaction tablet product, critical process parameters including compaction pressure[3], compaction speed[4] and powder particle size[5] have great impact on the quality of final product. Throughout all these processes, pharmaceutical material science plays an increasingly important role. As the FDA puts more emphasis on the concept of quality by design (QbD) [6], the development of a drug product has moved from

fostering empirical practice such as trial-and-error approach to understanding the fundamental knowledge of materials and process parameters. With mechanistic understanding of material properties, pharmaceutical scientists can not only decode and solve an existing problem related to poor pharmaceutical properties but also develop new materials with desired properties.

The overall objective of this thesis research is to demonstrate pharmaceutical materials science as a powerful tool to understand compaction behavior of bulk drug powder and improve physical properties and manufacturability of drug product. Two classic antihistamines drugs, loratadine and desloratadine, were utilized as model compounds. This thesis research covers the following aspects of pharmaceutical materials science:

(1) Understanding macroscopic compaction behavior of drug bulk powders via microscopic crystal structure and intermolecular interaction analysis

(2) Developing new solid states of drugs with improved physicochemical properties and manufacturability by crystal engineering approach

In this work, we gave an explicit explanation on the distinct compaction behaviors between loratadine and desloratadine, designed a new salt of loratadine with enhanced solubility and sweet taste to enable the development of a chewable tablet formulation. The mechanistic understanding of diverse compaction properties of drugs and the efficient approach to enable the development of chewable tablets through crystal engineering can be applied to solve problems encountered with other drugs.

1.2 Loratadine and Desloratadine

Loratadine (Lor) and desloratadine (Des) are classic H1-receptor antihistamines for the relief of allergic diseases such as allergic rhinitis and urticaria.[7] They are competitive inverse agonists of the H1 receptor that have relatively high specificity and can stabilize the receptor in inactive state.[8] They are classified as second generation H1-receptor antihistamines due to non-sedating advantages over the first generation products.[9] Compared to the first-generation drugs, which rapidly get into central nervous system, Lor and Des have higher peripheral selectivity and do not cross the blood-brain barrier.[10] Thus, they seldom cause side effect like drowsiness or somnolence and can be taken by patients of special occupation including pilots or drivers.[11]

Lor was patented in 1981[12] and brought to market in 1988 by Schering-Plough. It was first developed as a derivative of azatadine with tricyclic structure.[13] The ester chain was introduced as its N-substituent with the intention to reduce penetration into brain.[13, 14] Lor reaches peak blood concentration 1.5 h after oral dosing and rapidly metabolized by liver through first pass effect.[15] The major active metabolite of Lor is descarboethoxyloratadine, which was four times more potent than Lor and subsequently developed as Des.[16] The elimination half-life is 8–14 hours for Lor and 17–24 hours for Des, which leads to the 24-hour duration of action when Lor is administered.[15, 17] FDA approved the over-the-counter (OTC) status of Lor in 2002. The commercial product of Lor, Claritin, has become one of the most successful OTC products.[18, 19]

Des was patent in 1984[20] and brought to market in 2001 by Schering-Plough. Des is the primary active metabolite of Lor. It is a classic example of discovering a new drug from investigating the metabolites of an existing drug. Similar to Lor, Des exhibits a short onset time and reaches peak blood concentration 3h after dosing.[21] The longer elimination half-life, less extensive first pass metabolism and higher potency compared to Lor supports its once daily dosing and makes it a good alternative to Lor.[22-24]

1.3 Tablet and tablet strength

Tablet is the most common dosage form for drug administration.[25] It will continue to be the mainstay of drug therapy because of the several advantages, including better stability of drugs, ease of administration, lower cost of manufacturing, and better patient compliance.[26] According to different absorption site and intended clinical use, the drug release mode can be controlled, leading to various types of tablets: immediate release tablets, sustained/controlled release tablets, delayed release tablets, buccal and sublingual, chewable tablets, effervescent tablets, and orally disintegrating tablets.[27] Several tablet types, including chewable tablet and orally disintegrating tablet, have been marketed for Lor and Des.

A successful tablet product should meet several requirements, including good physical and chemical stability of drugs, uniform distribution of drugs, high purity, appropriate mechanical strength, appropriate drug release profile, and good manufacturability.[28]

In term of the requirement of tablet strength, a tablet must be strong enough to withstand the stress and crushing during handling, packaging and shipping and to avoid unacceptable friability and reduced drug dose.[29] On the other hand, unnecessarily excessive strength leads to slower tablet disintegration and drug release, which is not suitable for treating emergency cases needing fast drug release.[30, 31]

Developing tablets with appropriate strength is a challenging task because tablet properties vary significantly with the change of materials. For example, tablet strength depends on mechanical properties of API as well as particle size. Polymorphs of the same drug, i.e., same molecular structure but different crystal packings, may exhibit distinct tableting properties.[32] Variations in initial particle size of bulk powders also may significantly influence tableting behavior.[33] Thus, a comprehensive understanding of the structure-property relationship at different length scales, ranging from single molecule to crystal lattice to the bulk powder and to the finished tablet, is beneficial to develop tablet products of high quality and provide solutions to tabletability related problems.

1.4 Structure-property relationship

For pharmaceutical materials, pertinent properties include physicochemical properties, mechanical properties (elasticity, plasticity, brittle), particulate properties, surface properties, powder tabletability, powder flowability, powder cohesion and sticking.[2] These properties are affected by structures at molecular (chemical composition of

molecules), crystal (crystal structure, bonding strength and bonding patterns)[34, 35], granular (particle size and shape)[36], bulk powder (powder surface structure)[37], and finished drug products (tablet porosity)[38] levels.

Tablet compaction is a process of material consolidation, which depends on the mechanical properties and deformation mechanisms of the material. The most common deformation mechanisms include elastic deformation, plastic deformation, and fragmentation. Most pharmaceutical materials exhibit all three types of deformation depending on the pressure applied. Typically, elastic deformations take place under a low compaction pressure. For perfectly elastic materials, particles recover to original shape upon the removal of stress and the interparticular contact areas reduce to point contacts after decompression process. Thus, high elasticity deteriorates powder tabletability.[39] On the contrary, the permanent plastic deformation leads to large contact and bonding area, which is necessary for tablet formation.[26] Higher plasticity generally leads to superior compaction properties of drugs.

It has been shown that plasticity has strong relationship with crystal packings.[32, 34, 35] The presence of active slip planes is one of the leading contributors to plasticity of crystals. Slip planes are crystallographic planes in the crystal exhibiting weak interplanar interactions. They are typically of the highest molecule density and largest *d*-spacing when compared to other planes in the same crystal structure. The lower interaction energy and smoother surfaces of slip planes favor more facile slip, which results in higher plasticity and better tabletability of pharmaceutical materials.[40, 41]

This correlation between crystal structure and mechanical properties has been verified in a new context by comparing the compaction behavior of Lor and Des in the Chapter 2 of this thesis.

1.5 Crystal engineering

Understanding the relationships between structure and properties of materials is a critical first step. The next step is to use such knowledge to design materials with desired properties. Crystal engineering is a powerful tool to accomplish this.[42]

Crystal engineering is the design of new solid form with desired properties based on the understanding of intermolecular interaction.[43] The main intermolecular interactions in crystal engineering are hydrogen bonding and van der Waals interactions.[44] These intermolecular interactions link critical functional groups in different molecules together and form supramolecular synthons. In this way, new solid forms of a molecule can be synthesized by judicious selection of coformers with desired properties and functional groups for synthon formation.

Crystal engineering has recently been utilized to address common problems of pharmaceutical compounds caused by poor physicochemical properties such as physical and chemical stability, solubility, dissolution, bioavailability, and mechanical properties.[45-48] In 2015, the first cocrystal drug Entresto was approved by FDA for the treatment of chronic heart failure. This cocrystal is a trisodium hemipentahydrate

cocrystal-salt containing Valsartan and Sacubitril in 1:1 molar ratio[49], exhibiting superior efficacy and reduced side effect compared to pure Valsartan.[50] This example demonstrates the potential of crystal engineering as a promising approach to not only enable the more robust manufacturability but also drugs with better clinical outcomes.

Lor and Des also have some pharmaceutical deficiencies, such as poor aqueous solubility.

1.6 Structure of thesis

Chapter 2

In Chapter 2, we tried to explain why Lor exhibited much higher tabletability than Des over the typical tableting pressure range of 25-350 MPa. The more superior tabletability of Lor is explained by its both larger bonding area (BA) and higher interparticle bonding strength (BS). The larger BA of Lor is attributed to its higher crystal plasticity, which is determined both experimentally and computationally by energy framework calculation and topological analysis. Higher BS is attributed to the significantly higher dispersive component of the surface energy of Lor than that of Des. This work provides new insights into molecular origins of both BA and BS, which can be applied to guide future crystal engineering to improve mechanical properties and tableting performance of drugs.

Chapter 3

In Chapter 3, we synthesized the first multicomponent crystalline form of Lor with artificial sweetener saccharin. The new salt exhibits sweet taste, enhanced solubility and dissolution rate, as well as acceptable physical stability, which facilitates the development of a chewable tablet formulation. The simultaneous release of loratadine and sweetener without problems of physical separation between sweetener and drug during manufacturing process makes it effective in masking the bitter taste of Lor. We identified a compaction pressure window by applying friability and chewing difficulty index requirement. This example shows the usefulness of sweet salt formation in the development of a chewable tablet product of a drug with poor solubility and unpleasant taste.

CHAPTER 2

Molecular insights into the distinct compaction behaviors of two structurally similar antihistamine drugs: loratadine and desloratadine

2.1 Introduction

Loratadine (Lor) and desloratadine (Des) (Fig. 2.1) are second generation H1-receptor antihistamines widely used for the relief of allergic rhinitis and urticaria[1]. They have high peripheral selectivity and do not readily cross the blood-brain barrier, leading to non-sedating advantages over first generation drugs that have side effects, such as drowsiness and somnolence [2]. Lor was first developed as a derivative of tricyclic azatadine. The ester chain on Lor possibly accounts for its low penetration into brain[3, 4]. Lor reaches peak blood concentration 1.5 h after oral dosing and rapidly metabolized by liver through first pass effect[2, 5, 6]. The major active metabolite of Lor, descarboethoxyloratadine or Des, was subsequently developed into a new drug. FDA granted Lor over-the-counter (OTC) status in 2002, which has become one of the most successful OTC products under the brand name, Claritin[7, 8]. Des is a successful example of discovering new drugs from carefully investigating metabolites of existing drugs. Compared to Lor, Des exhibits longer elimination half-life, less extensive first pass metabolism, and higher potency[9-11]. Thus, Des is a useful alternative to Lor[12].

Most commercially available products of Lor and Des are tablets. Tablets remain a preferred dosage form because of their physical and chemical stability, ease of administration, high manufacturing efficiency, and low manufacturing cost[13]. One of the criteria for a successful tablet product is appropriate mechanical strength so that they are strong enough to withstand crush during handling and storage but not too strong to cause

problems such as slow drug release[14], difficulty with chewing[15] and prolonged disintegrating time[16]. This is relevant to both Lor and Des because they have orally disintegrating tablet and chewable tablets on the market.

Despite their similar molecular structures, Lor and Des exhibited significantly different tabletability, where tablet tensile strength of Lor is more than two times that of Des over a wide range of compaction pressure. The large difference between tabletability of Lor and Des suggests their significantly different crystal mechanical properties[17-19]. Thus, Lor and Des present an opportunity to further advance the current state of understanding in the relationship between crystal structure and mechanical properties. Past efforts in this direction used anhydrate and hydrate crystals[20, 21], different polymorphs[22, 23], cocrystals [24, 25], and salts [26, 27]. Lor and Des pair is the first example of exploring crystal structure – mechanical property relationship using a drug and its metabolite.

2.2 Materials and Methods

2.2.1 Materials

Both Loratadine and Desloratadine were purchased from Wuhan Biocar Bio-pharm Co. Ltd. (Wuhan, Hubei, China). Microcrystalline cellulose (MCC; Pharmacel 102) was provided by DFE Pharma (Goch, Germany). All materials were used as received.

Deionized water, formamide (Sigma−Aldrich, St. Louis, MO) and diiodomethane (DIM; Sigma−Aldrich, St. Louis, MO) were all reagent grade.

2.2.2 Methods

2.2.2.1 Powder X-ray Diffractometry (PXRD)

A wide-angle X-ray diffractometer (X'Pert Pro; PANalytical Inc., West Borough, MA) with Cu Kα radiation (45 kV and 40 mA, wavelength of 1.54059 Å.) was used to collect X-ray diffraction patterns at ambient temperature. Discs of Lor and Des were prepared by compressed at 200 MPa and the flat surface of discs were scanned between 5 and 35° 2θ with a step size of 0.017° at 1s/step. Theoretical PXRD patterns were calculated from crystal structures (CSD refcodes: BEQGIN for Lor and GEHXEX for Des) using Mercury (V.3.10, Cambridge Crystallographic Database Centre, Cambridge, UK).

2.2.2.2 Thermal Analysis

Thermal stability was analyzed using thermogravimetric analysis (TGA) and differential scanning calorimetry (DSC). For TGA, a thermogravimetric analyzer (Q500; TA Instruments, New Castle, DE) was used. Approximately 3 mg of each sample was placed in an open aluminum pan and heated from room temperature to 250℃ at 10℃/min under dry nitrogen purge (75 mL/min). For DSC, a differential scanning calorimeter (Q1000, TA Instruments, New Castle, DE) was used. Approximately 3 mg of sample was loaded into Tzero hermetically sealed aluminum pans and heated from room temperature

to 175 °C at a heating rate of 10 °C/min under a continuous nitrogen purge at a flow rate of 25 mL/min. DSC cell parameter was calibrated with indium for heat flow, indium and cyclohexane for temperature.

2.2.2.3 Dynamic Water Vapor Sorption Isotherm

Isothermal water sorption profiles were obtained from an automated vapor sorption analyzer (Intrinsic DVS, Surface Measurement Systems Ltd., Allentown, PA, USA) at 25°C with nitrogen flow rate of 50 mL/min. Each sample was equilibrated at a series of RHs, from 0% to 95% in 5% increments, and sample weight was monitored by a micro balance. Once one of two equilibration criteria, $dm/dt \leq 0.003\%$ or maximum equilibration time of 6h, was reached, the relative humidity (RH) was changed to the next target value by controlling flow rates of the dry and wet lines of nitrogen gas.

2.2.2.4 Powder Compaction

Lor and Des powders were first undergone sieve cut of 125-180 μm to control the particle size to minimize unwanted influence on the tablet behavior of powders. Sieved powders were observed under a polarized light microscope (Eclipse e200; Nikon, Tokyo, Japan) to compare their particle size. Formulations containing 25% (w/w) either of Lor or Des and 75% (w/w) MCC PH102 were mixed in a glass bottle and the bottle was blended on a mixer (Turbula, Glen Mills Inc., Clifton, NJ) at 49 rpm for 4 min.

A material test machine (model 1485, Zwick/Roell, Ulm, Germany) was used to explore the tableting behavior of Lor, Des and their formulations. Tablets with approximately 150 mg of weight were prepared separately over the 10-300MPa compaction pressure range at a punch speed of 5 mm/min (8 mm flat faced punch). Tablets were relaxed under ambient conditions for at least 24h before measuring their dimensions and diametrical breaking force.

2.2.2.5 Powder true density and tablet porosity

Powder true density was measured using a helium pycnometer (Quantachrome Instruments, Ultrapycnometer 1000e, Byonton Beach, Florida). Approximately 1 g accurately weighed sample was placed into a sample cell (10 mL cell volume). A total of 100 measurement cycles were run unless the coefficient of variation of five consecutive measurements was < 0.005%. The last five measurements were used to calculate an average and standard deviation of true density. Tablet porosity (ε) was calculated using Eq. (2.1):

$$\varepsilon = 1 - \frac{\rho}{\rho_t} \qquad (2.1)$$

where ρ and ρ_t are tablet density and powder true density, respectively.

2.2.2.6 Tabletability analysis

Tablet diametrical breaking force was determined using a texture analyzer (TA-XT2i; Texture Technologies Corporation, Scarsdale, NY) at a speed of 0.01 mm/s with 5 g trigger force. Tablet tensile strength was calculated from Eq. (2.2)[28]:

$$\sigma = \frac{2F}{\pi D h} \tag{2.2}$$

where F, D, and h are the breaking force (N), tablet diameter (mm), and thickness (mm), respectively.

2.2.2.7 Compressibility analysis

Compressibility is the ability of a powder to undergo a reduction in volume as a result of an applied pressure, represented by a plot of tablet porosity against compaction pressure.[29] Compressibility data was analyzed using Heckel equation (Eq. 2.3)[30, 31] and Kuentz-Leuenberger (Eq. 2.4)[32]:

$$-\ln \varepsilon = KP + A \tag{2.3}$$

$$P = \frac{1}{C}\left[\varepsilon - \varepsilon_c - \varepsilon_c \ln\left(\frac{\varepsilon}{\varepsilon_c}\right)\right] \tag{2.4}$$

where ε and P represent tablet porosity and compaction pressure respectively. The reciprocal of K, named mean yield pressure (P_y) and 1/C correspond to material plasticity. A lower P_y or 1/C value corresponds to higher material plasticity. Linear portion ($R^2 > 0.99$) of the Heckel plot in the middle compaction pressure region were used for calculating P_y.

2.2.2.8 Compactibility analysis

Compactibility is the ability of a material to produce tablets with sufficient strength under the effect of densification, which is represented by a plot of tablet tensile strength against tablet porosity. Compactibility data was analyzed using Eq. 2.5: [23]

$$\sigma = \sigma_0 e^{-a\varepsilon} \qquad (2.5)$$

where σ is tablet tensile strength, ε is tablet porosity, σ_0 is the tensile strength of the tablet at zero porosity and *a* is an empirical constant describing the sensitivity of σ to changes in ε.

2.2.2.9 Contact angle and surface energy

Compacts prepared by compressing Lor and Des powders at 300 MPa were used for contact angle measurement using a goniometer (MAC-3, Kyowa Interface Science Co. Ltd., Japan) by the sessile drop method. A drop of approximately 2 μL probe liquid was gently placed on the surface of the tablet using a syringe dispenser. The image of the liquid drop was recorded every 67 ms for 60 s using a high-speed camera. The angle between the sample surface and the tangent line at the edge of the drop was determined using image analysis software, FAMAS3.72 (Kyowa Interface Science Co. Ltd., Japan). Three measurements were made at different locations on each tablet, and the mean and standard deviation were calculated.

Surface energy of Lor and Des were calculated using Owens/Wendt theory (harmonic mean method).[33] Contact angle data can be plotted in the form of Eq. (2.6):

$$\frac{\gamma_L(1+\cos\theta)}{2\sqrt{\gamma_L^D}} = \sqrt{\gamma_S^P} \times \sqrt{\frac{\gamma_L^P}{\gamma_L^D}} + \sqrt{\gamma_S^D} \qquad (2.6)$$

where γ_L^D = dispersive component of the surface tension of the wetting liquid, γ_L^P = polar component of the surface tension of the wetting liquid, γ_S^D = dispersive component of the surface energy of the solid, γ_S^P = polar component of the surface energy of the solid, γ_L= total surface tension of the wetting liquid and θ = the contact angle between the liquid and the solid. The surface energy parameters of reference liquids are summarized in Table 2.1. From the fitting line of the plot of $\frac{\gamma_L(1+\cos\theta)}{2\sqrt{\gamma_L^D}}$ vs. $\sqrt{\frac{\gamma_L^P}{\gamma_L^D}}$, the γ_S^P can be calculated from the slope and γ_S^D can be calculated from the intercept. The total surface energy of solid is the summary of dispersive and polar component.

2.2.2.10 Structure Visualization and Topology Analysis

The crystal structures of Lor (BEQGIN) and Des (GEHXEX) were visualized using Mercury (4.1.0, CCDC, Cambridge, UK). The quantitative layer topology in crystal structure was analyzed using CSD Python program.[34]

2.2.2.11 Energy framework

The intermolecular interaction energy was calculated based on B3LYP-D2/6-31G(d,p) electron densities model using CrystalExplorer (v17.5, University of Western

Australia)[35] and Gaussian09. The hydrogen positions were normalized to standard neutron diffraction values before the calculation. The energy framework was constructed based on the crystal symmetry and total intermolecular interaction energy, including electrostatic, polarization, dispersion, and exchange-repulsion components with scale factors of 1.057, 0.740, 0.871, and 0.618, respectively.[36] The intermolecular interaction with a intermolecular distance more than 3.8 Å was neglected.[37] In the energy framework, cylinder thickness is proportional to the intermolecular interaction energy and interactions energy below a certain energy threshold are omitted for clarity.

2.3 Results and Discussion

2.3.1 Solid state properties

Prior to compaction, solid state characterizations of the bulk powders of Lor and Des were carried out to ensure the phase purity and stability of powders. The PXRD patterns of the bulk powders of Lor and Des matched well with the PXRD patterns calculated from their corresponding single crystal structures (Fig. 2.2), confirming the high phase purity of bulk powders. For Des, the slight shift of experimental peaks to lower 2θ angles is attributed to thermal expansion of unit cell since experimental PXRD data were collected at 298 K but the crystal structure was solved at 100 K [38]. A majority of sharp peaks can still be observed in the PXRD patterns of Lor and Des tablets compressed at 300

MPa, indicating phase stability of both crystals against compaction. The differences in peak intensity are attributed to the preferred orientation.

The DSC thermograms (Fig. 2.3a) show that Lor exhibited a lower melting point (134.43 °C) and heat of fusion (81.41 J/g) than those of Des (155.28 °C, 137.5 J/g). No significant weight loss of Lor and only 2.0% weight loss of Des were observed at 200 °C in TGA thermograms (Fig. 2.4). The constant sample weight before melting temperature suggests no sublimation occurred before melting event took place. Both Lor and Des are not hygroscopic because less than 1.0% weight was gained at 95% RH (Fig. 2.3b). The slightly higher moisture sorption of Des is consistent with its higher aqueous solubility than Lor.[39]

2.3.2 Compaction properties of Lor and Des bulk powders

The tabletability of Lor is always better than that of Des over the entire compaction pressure range and nearly 3-fold at high compaction pressures (Fig. 2.5a). The slight decrease in tensile strength of Lor and Des at high compaction pressure range (> 250 MPa) suggest possible overcompression, which is usually caused by excessive elastic recovery that induces macro defects in tablet[40].

The tablet tensile strength is the net effect of the interplay between bonding area (BA) and bonding strength (BS)[41]. Since particle sizes were comparable (Fig. 2.6), the

significantly better tabletability of Lor cannot be explained by difference in particle size. However, the much better tabletability can be explained by its higher apparent BS, which is shown by its greater tensile strength at zero porosity (σ_0) (Fig. 2.5b). Moreover, porosity of Lor tablet is lower than Des tablet under the same compaction pressure (Fig. 2.5c), indicating Lor is more plastic and compressible than Des. This is confirmed by the lower P_y of Lor (161±6 MPa) than Des (256±10 MPa) and the lower plasticity parameter $1/C$ of Lor (382±47 MPa) than that of Des (871±58 MPa). The lower tablet porosity or Lor corresponds to larger BA. Therefore, both larger BA and higher BS explains the significantly higher tabletability of Lor than Des.

When mixed with 3 parts of MCC (75%, w/w), the compressibility profiles of the two formulations were nearly identical (Fig. 2.8a). This is reasonable because consolidation of the mixtures was dominated by the plastic MCC. However, the higher tabletability and compactibility of Lor than Des (Figs. 2.5a, 2.5b) still led to higher tabletability (Fig. 2.7a) and compactibility (Fig. 2.7b) of Lor formulation. Thus, the large difference between tabletability of Lor and Des have an impact on the tabletability of formulations even only 25% of the drugs were present.

2.3.3 Structural origin of differential crystal plasticity

The crystal structures were analyzed to understand the different mechanical properties of Lor and Des. Key crystallographic parameters of Lor and Des are summarized in Table 2.2. It has been well established that organic crystals exhibiting active slip planes or columns, featured with strongly intra-layer/column interactions but weak inter-layer/column interactions and smooth layer/column surfaces, favor the plastic deformation[42]. Such plastic crystals usually exhibit larger BA and, therefore, better compressibility and tabletability than harder crystals[25, 43, 44]. Although both Lor and Des contain two nitrogen atoms, no strong hydrogen bond of N-H···N is observed in them. In Lor crystal, dimers connected through weak hydrogen bonds of C-H···O=C (3.380 Å) assembled into infinite 1D chain along the *c* direction (Fig. 2.9a). Such 1D chains assemble into flat layers with relatively large interlayer separation. This structure implies high plasticity. In Des, 1D infinite zigzag chains are formed through C-H···N (3.357 Å) weak hydrogen bonds (Fig. 2.9b), which stack to form 2D layers through C-H···π (3.599 Å) interactions along the *bc* plane (Fig. 2.9f).

Neighboring chains in Lor and layers in Des are simply arranged in the close-packed fashion, without strong hydrogen bonds or aromatic stacking between adjacent chains or layers.[38, 45] Therefore, molecular packing in both crystals is dictated by dispersive forces. The calculated intermolecular interaction energies, confirm that the dispersive interaction is the major bonding energies for both Lor and Des (Fig 2.10, Table 2.3). In addition, the larger lattice energy of Des (286.8 kJ/mol) than Lor (276.4 kJ/mol) is in

agreement with the higher melting point (155 °C vs 134 °C) and density (1.373 vs. 1.364 g•cm^{-3} at 100 K) of Des. It was shown before that visualization of crystal structure alone can lead to erroneous assignments on slip planes and predictions of mechanical properties. In contrast, an integrated energy framework calculations and topology analysis is much more reliable [42, 46]. The energy framework suggested that (1 0 $\bar{1}$) is the primary slip plane for Lor. The much larger intralayer bonding energy (-218.7 kJ/mol) than its interlayer bonding energy (-57.7 kJ/mol), and positive interlayer distance (+0.1 Å) suggested, both energetically and topologically, that (1 0 $\bar{1}$) plane is an active slip plane (Fig. 2.9c, 2.9e). However, no clear active slip plane was identified in Des because all layers are interlocked. The most probable slip plane, (1 0 $\bar{1}$), determined by topology analysis exhibits interdigitation with a negative interlayer distance of -0.72 Å (Fig. 2.9d). The energy framework of Des (Fig. 2.9f) suggested that (0 0 1) is the most energetically favorable for slip but these planes are interlocked with a greater degree of interdigitation (interlayer distance -1.14 Å). Thus, the structure analysis shows that the plasticity of Des is much lower than that of Lor, which is consistent with the lower P_y of Lor from the Heckel analysis (Fig. 2.9d) and lower 1/*C* from the K-L analysis.

2.3.4 Relationship between interparticlular bonding strength and surface energy

Surface energy has been thought to strongly influence powder compaction behavior by affecting bonding strength[14, 47, 48]. Such a correlation was examined in this work, where

surface energy of Lor and Des was quantified by analyzing contact angles with three probe liquids using the Owens/Wendt theory (Fig. 2.11, Table 2.4).

The total surface energy of Des is higher than that of Lor. However, the composition of surface energy is radically different between Lor and Des. Lor exhibits a greater fraction of dispersive surface energy while Des exhibits a greater fraction of polar surface energy. At the contact points in a compressed tablet, molecules are separated only by a molecular distance[14]. Dispersive forces are effective at this distance for molecular solid[49]. For Lor and Des, no strong hydrogen bond could be found in their crystal structure and their whole structures were linked mainly by weak dispersive interaction. It should be noted that weak hydrogen bonds are dispersive interactions in nature, except for the directionality[50]. In addition, polar interactions play a more important role at the liquid-solid interface than at the solid-solid interface, which explains the higher moisture sorption (Fig. 2.3b) and aqueous solubility of Des than Lor [39]. However, it was suggested that the dispersion forces dominate polar forces at the solid-solid interface in tablet[49, 51]. The correspondence between larger dispersive surface energy and higher BS of Lor than those of Des supports this view, which can be readily understood by considering characteristics of polar interaction and the random orientation of particles in tablet. Polar interactions, such as hydrogen bonds, require stringent directionality to be effective. Their strength and directionality direct molecular packing in crystals, which is essential for designing crystals by modifying molecular structures or selecting co-crystalizing molecules[52-54]. That is also

why crystals with structures dominated by more polar interactions tend to have larger lattice energy and melting point, as in the case of Des. However, such directionality requirement can hardly be met at the contact points between particles in tablet because particles are randomly packed. Therefore, the total contribution by polar interactions to BS is low. This is an important hypothesis that deserve further exploration.

2.4 Conclusion

Despite similar molecular structures, Lor and Des exhibited very different mechanical properties and tableting behavior. The significantly higher tabletability of Lor bulk powder than that of Des is attributed to its both larger bonding area and apparent bonding strength. The larger bonding area of Lor is a result of its higher plasticity, which is established at molecular level by energy framework and topology analysis. The greater bonding strength of Lor is attributed to its much larger dispersive forces than Des. This study reveals new insights into the molecular origin of bonding area and bonding strength that is critical for understanding tabletability. Such fundamental understanding paves the way for future design of crystals exhibiting desirable mechanical properties and tableting behavior through crystal engineering.

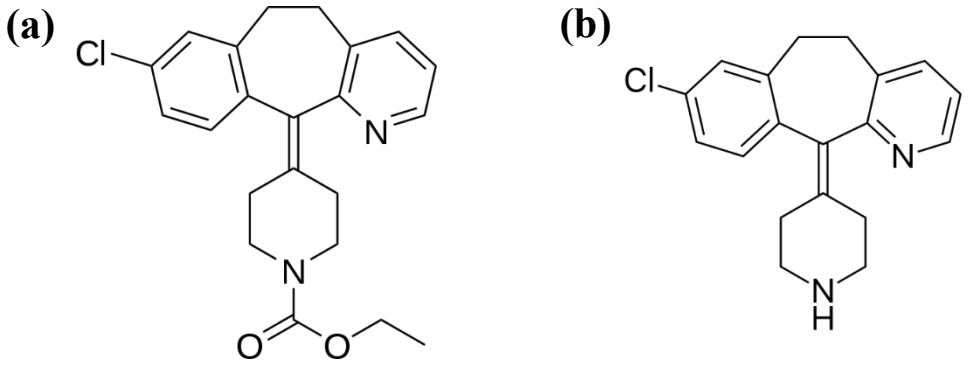

Figure 2.1 Chemical structures of (a) Lor and (b) Des

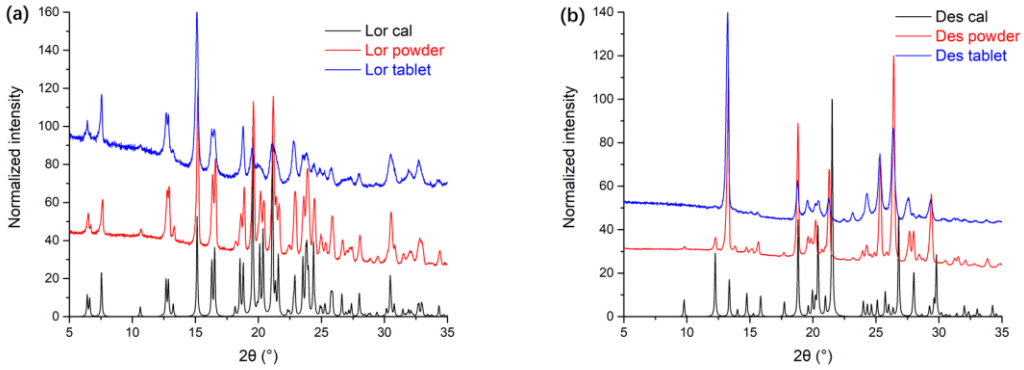

Figure 2.2 Powder X-ray diffraction patterns (calculated, bulk powder and tablet surface) of (a) Lor and (b) Des.

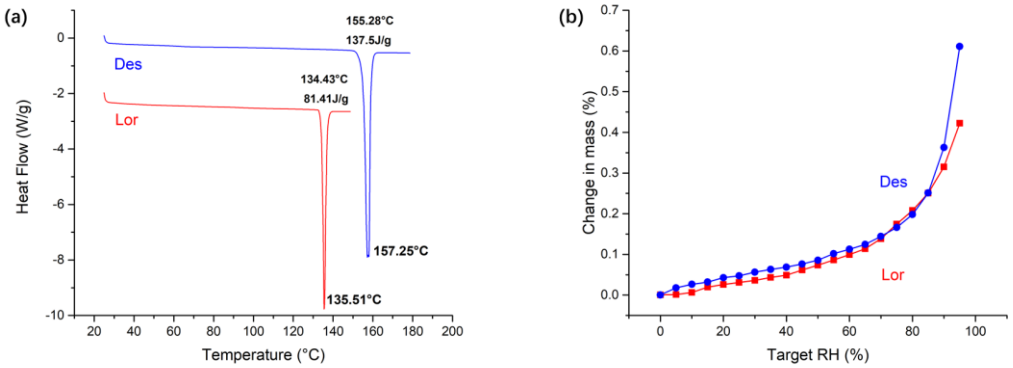

Figure 2.3 Physicochemical properties of Lor and Des: (a) thermal properties by differential scanning calorimetry and (b) moisture sorption isotherm at 25 ºC

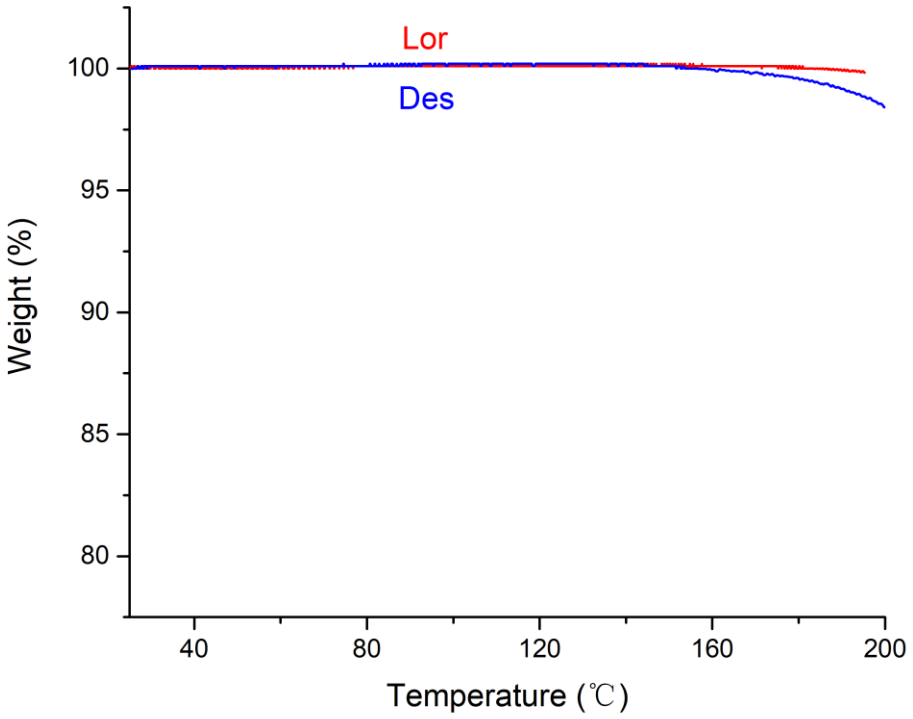

Figure 2.4 Thermogravimetric analysis thermogram of Lor and Des

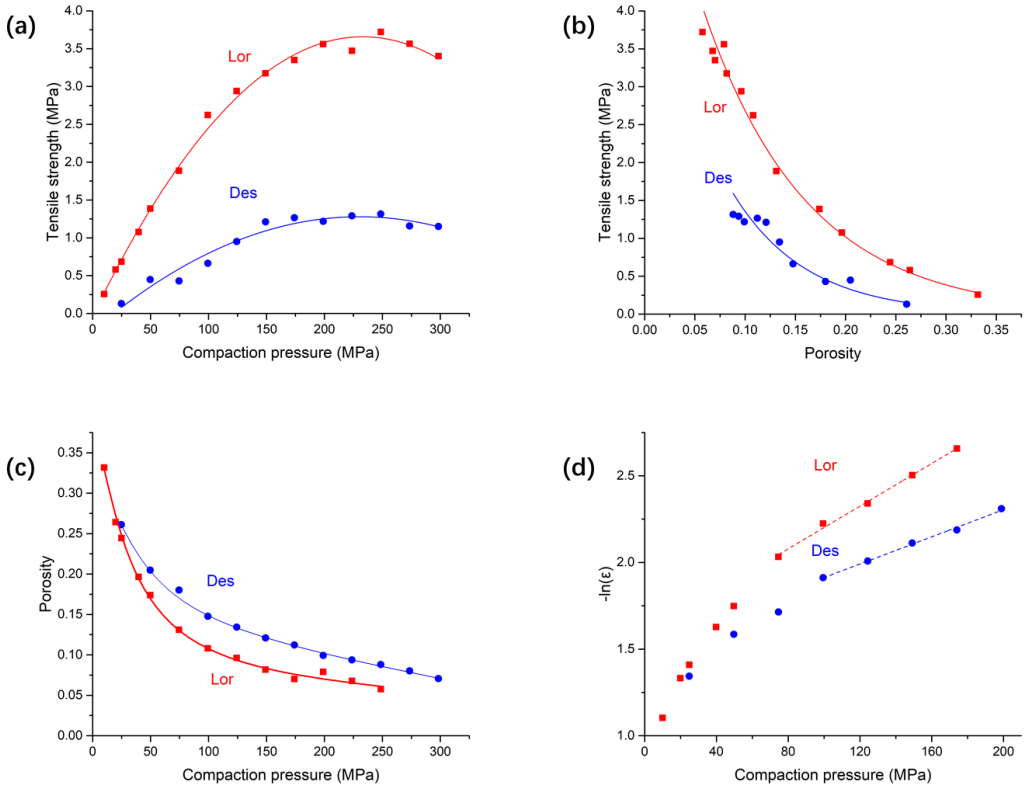

Figure 2.5 (a) Tabletability, (b) compactibility, (c) compressibility, and (d) Heckel analysis profiles of Lor and Des in bulk powder.

(a) **Lor**

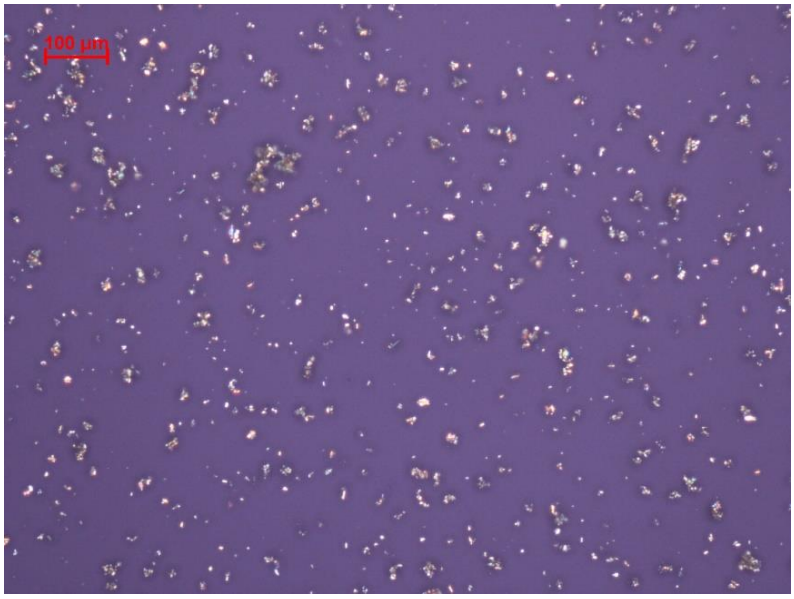

(b) **Des**

Figure 2.6 Pictures of (a) Lor and (b) Des powders under polarized light microscope

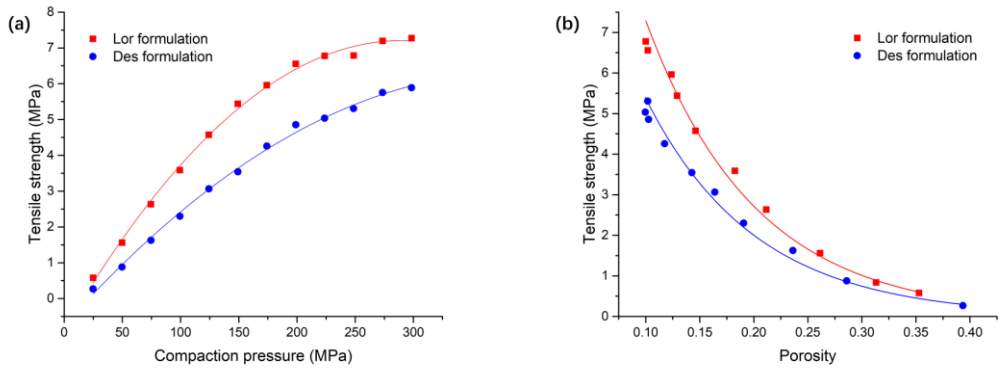

Figure 2.7 Compaction properties of Lor and Des formulations: (a) tabletability and (b) compactibility profiles. The formulation is comprised of 25% Lor/Des and 75% MCC (w/w)

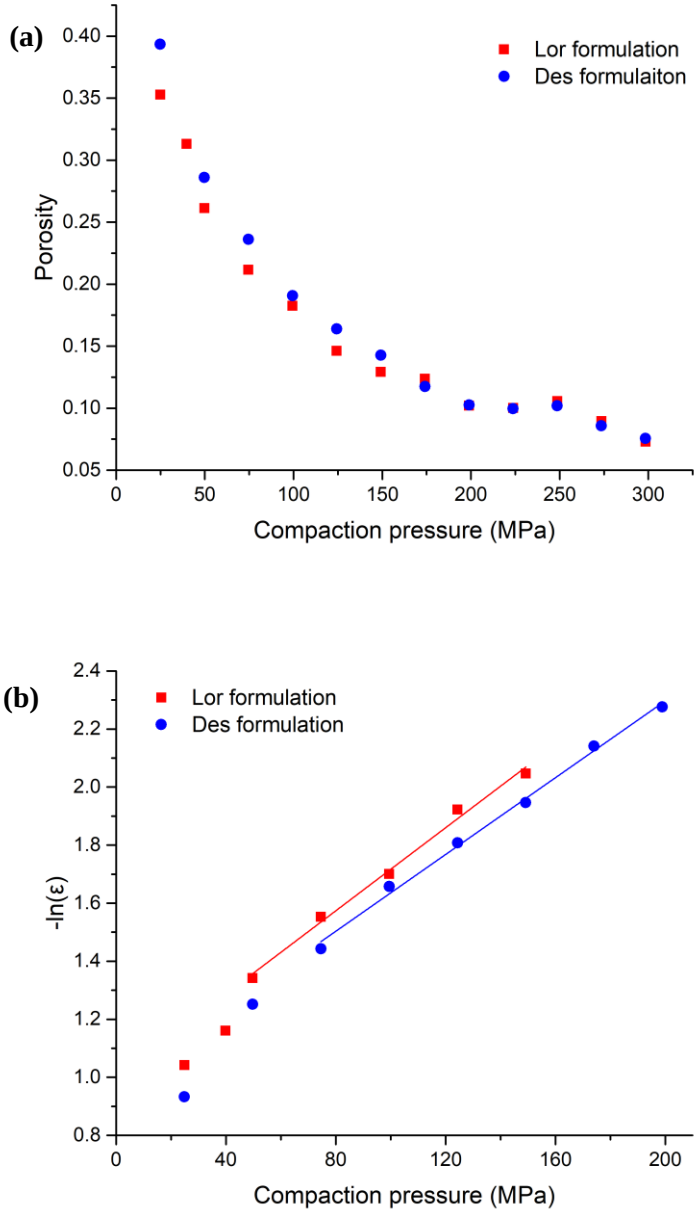

Figure 2.8 Compaction properties of Lor and Des formulations: (a) compressibility and (b) Heckel analysis profiles. The formulation is comprised of 25% Lor/Des and 75% MCC (w/w)

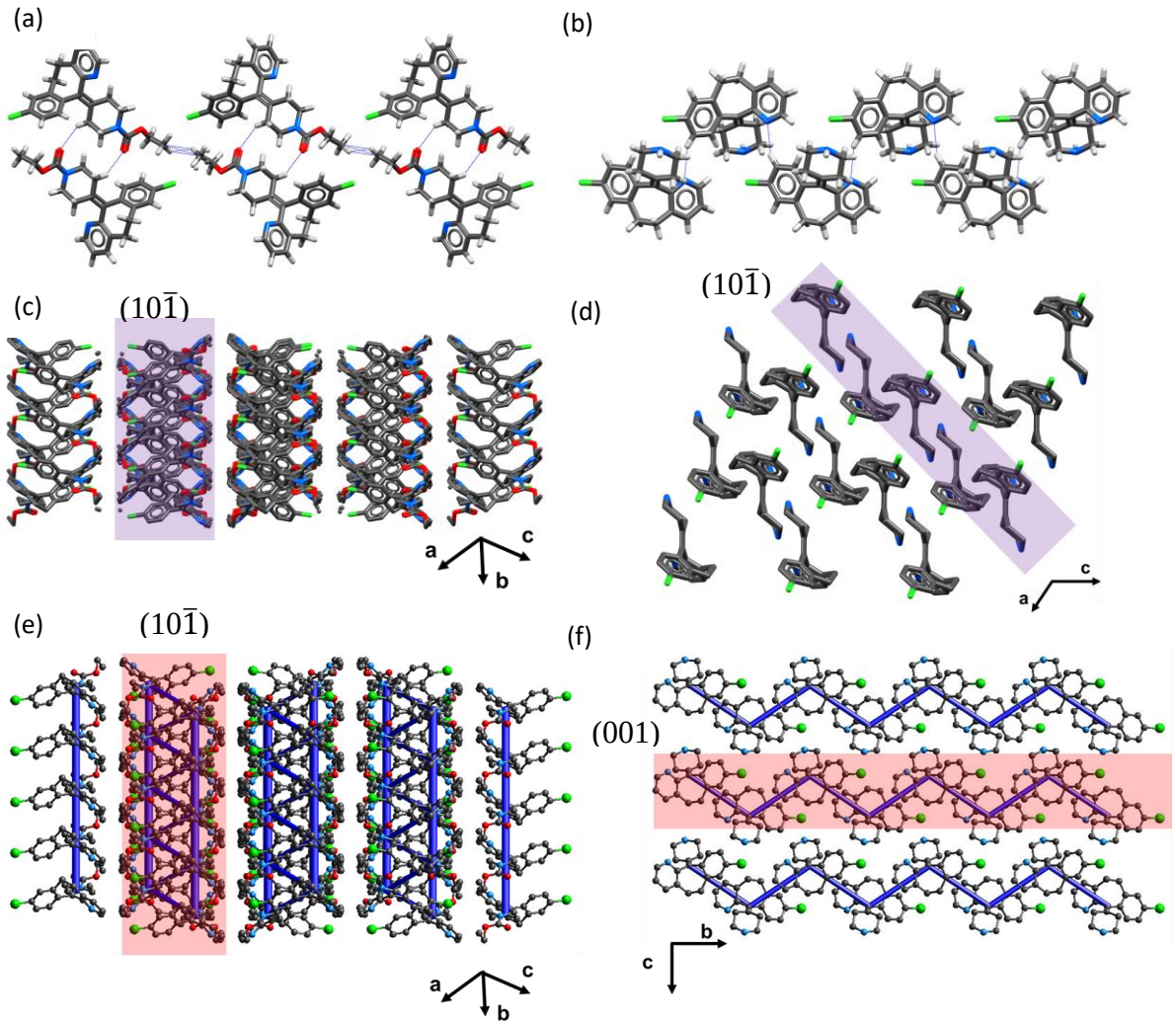

Figure 2.9 Comparison of packing patterns of Lor (a, c, e) and Des (b, d, f). Infinite 1D molecular chain observed in (a) Lor and (b) Des. The stereoview of the (c, d) packing arrangement patterns and (e, f) the energy framework. The thickness of each cylinder (in blue) represents the relative strength of intermolecular interaction. The energy threshold for the energy framework is set at −25 kJ/mol.

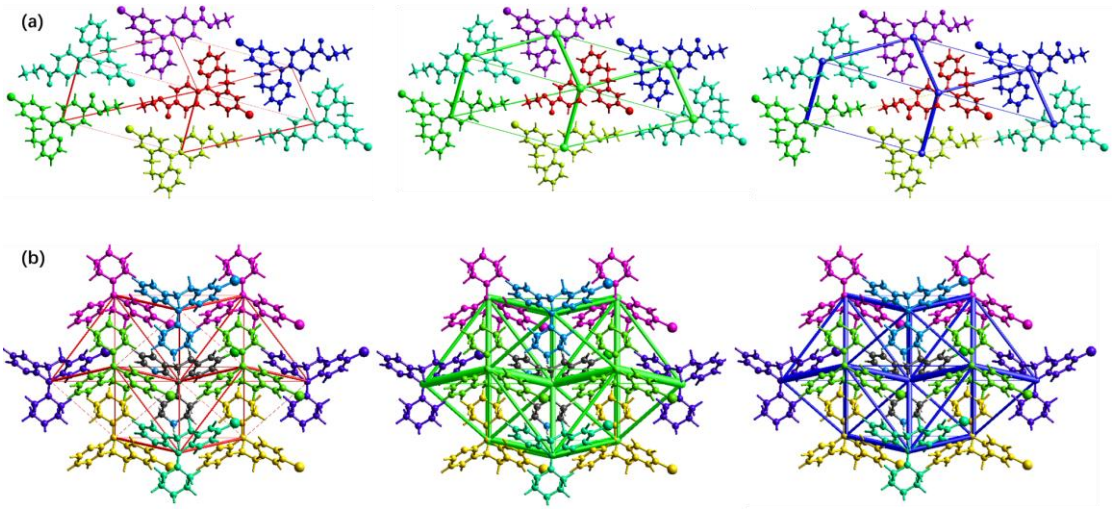

Figure 2.10 Energy frameworks of (a) Lor and (b) Des, the electrostatic, dispersion, and total energies are colored red, green, and blue, respectively, with cylinder thickness proportional to the magnitude of the interaction energy.

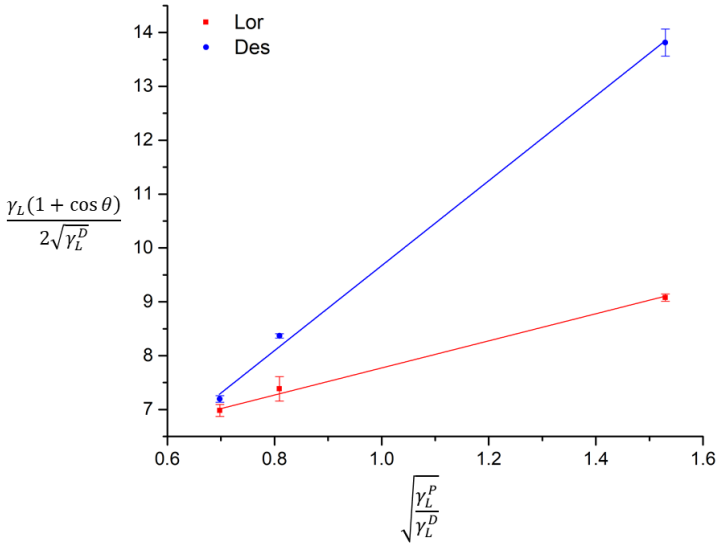

Figure 2.11 Owens/Wendt surface energy plot of Lor and Des. The unit of all surface energy is mJ/m^2

Table 2.1 Surface tension component of reference liquid.

Reference liquid	γ_L^D	γ_L^P	γ_L
Water	21.8	51	73
Formamide	39	19	58
DIM（Diiodomethane）	49.5	1.3	51

(unit: mN/m)

Table 2.2 Crystallographic parameters of Lor and Des

Compound	Lor	Des
Chemical formula	$C_{22}H_{23}ClN_2O_2$	$C_{19}H_{19}ClN_2$
Crystal system	Monoclinic	Monoclinic
Space group	C2/c	$P2_1$
a (Å)	28.299 (3)	6.934 (1)
b (Å)	4.993 (1)	11.998 (2)
c (Å)	29.137 (3)	9.469 (1)
β (°)	109.19 (1)	107.37 (1)
Z	8	2
Z'	1	1
Volume ($Å^3$)	3888.204	751.826
T (K)	283-303	100
R-factor	4.4	3.2
Density (g/cm^3)	1.308	1.373
CCDC	BEQGIN	GEHXEX

Table 2.3 Intermolecular interaction energies estimated using B3LYP-D2/6-31G (d,p) dispersion corrected DFT model. Both the total energy (E(tot)) and electrostatic (E(ele)), polarization (E(pol)), dispersion (E(dis)), and exchange-repulsion (E(rep)) components of the energy are listed. R indicated the distance between centers of mass of the pair of molecules.

Loratadine

	Symop	R	E_{ele}	E_{pol}	E_{dis}	E_{rep}	E_{tot}
	x, y, z	4.99	-7.1	-2.6	-80.6	35.6	-57.6
	-x, -y, -z	7.84	-12.1	-4.5	-32.8	20.2	-32.2
	-x, -y, -z	8.24	-10.3	-5.9	-36.1	22.0	-33.1
	-x, y, -z+1/2	17.59	-8.4	-0.2	-11.1	34.0	2.3
	x, -y, z+1/2	14.90	-1.3	-0.3	-5.7	3.3	-4.5
	-x+1/2, -y+1/2, -z	9.45	-4.9	-0.8	-23.5	11.1	-19.4
	-x+1/2, y+1/2, -z+1/2	10.68	-5.3	-1.5	-23.8	13.3	-19.1
	-x+1/2, -y+1/2, -z	8.41	-4.5	-0.8	-35.6	15.4	-26.8
	x, -y, z+1/2	14.69	-0.2	-0.1	-3.4	1.3	-2.4

Desloratadine

	Symop	R	E_{ele}	E_{pol}	E_{dis}	E_{rep}	E_{tot}
	-x, y+1/2, -z	8.07	-14.1	-3.5	-24.9	28.4	-21.7
	-x, y+1/2, -z	9.23	-1.4	-1.0	-25.0	12.9	-16.1
	-x, y+1/2, -z	7.27	-11.5	-1.7	-59.4	43.3	-38.5
	x, y, z	6.93	-7.0	-1.9	-40.2	18.5	-32.5
	x, y, z	9.93	-5.1	-1.8	-11.3	5.8	-12.9
	x, y, z	12.00	-2.5	-0.4	-6.1	5.8	-4.6
	-x, y+1/2, -z	9.47	-8.1	-1.2	-24.4	22.2	-17.1

Table 2.4 Surface energy composition of Lor and Des. The unit of all surface energy is mJ/m^2

Material	γ_S^D	γ_S^P	γ_S
Lor	28.35±1.54	6.05±0.67	34.40±2.21
Des	3.55±1.49	61.04±5.36	64.59±6.85

CHAPTER 3

Development of Chewable Loratadine Tablet Through Sweet Salt Formation

3.1 Introduction

Loratadine (Lor, Fig. 3.1a) is a second-generation non-sedating H_1 antihistamine[1]. It is now widely used as an over-the-counter drug for the relief of allergic disorders like seasonal allergic rhinitis[2]. Lor is a Biopharmaceutics Classification System (BCS) class II drug with poor water solubility and low dissolution rate in the physiological pH range[3]. Bioavailability data suggested that the low solubility and dissolution rate of Lor partly account for its high inter- and intra-subject variability of the pharmacokinetic parameters in humans[3-5]. In order to minimize variation and achieve consistent bioavailability, many techniques have been utilized to increase the solubility of Lor, including inclusion complexation[6], self-emulsifying system[7], solid dispersion[8], polymorph selection[9], and coamorphous system[10]. However, these approaches require sophisticated techniques or additional processing steps, which lead to high manufacturing cost. In addition, Lor presents unpleasant taste[11]. In this work, we aimed at simultaneously overcoming the poor solubility and dissolution rate, as well as unpleasant taste of Lor by crystal engineering.

Crystal engineering is a technique that designs new solid forms with desired properties based on the understanding of intermolecular interaction[12]. Crystal engineering has been utilized to address common problems of pharmaceutical compounds caused by poor physico-chemical properties[13-16]. Among all crystal engineering approaches, salt formation plays a significant role in pharmaceutical industry. More than fifty percent of currently marketed drugs are prepared in salt form[17]. With rational selection of

counterions, solubility, dissolution, physical stability, and chemical stability can be improved to enable oral administration of drugs[18]. However, no pharmaceutical Lor salts have been developed to overcome its poor solubility and dissolution rate, and unpleasant taste problems[19].

Currently, chewable tablet is a popular dosage form of Lor. Chewable tablet is an oral dosage form intended for patients who are unable or unwilling to swallow intact tablets. The advantages of chewable tablet form include ease of administration, overcoming swallow difficulty, elimination of need of water, and better compliance provided taste of the drugs can be successfully masked to deliver pleasant taste, which are highly desired for children and elderly[20, 21]. The taste masking strategy employed in the currently marketed chewable tablet is to physically mix sweeteners and flavors with other formulation components. However, physical separation between the drug and sweetener during manufacturing process can reduce the effectiveness of taste masking. Thus, the simultaneous release of drug and sweetener by a sweet salt of Lor is highly attractive for chewable tablet development. This can be achieved through salt or cocrystal formation with artificial sweeteners[22, 23].

Lor contains a pyridine nitrogen atom, which can accept a proton[24]. In this study, we discovered a new sweet crystal with saccharin (Sac, Fig. 3.1b), which is a strong acid exhibiting strong tendency to donate its amide proton. We hypothesized that proton transfer can occur to facilitate the formation of a sweet salt between Lor and Sac and, if

successfully prepared, such a sweet salt can be used to develop a chewable tablet formulation of Lor.

3.2 Materials and Methods

3.2.1 Materials

Loratadine (Lor; Wuhan Biocar Bio-pharm Co. Ltd., Wuhan, Hubei, China), saccharin (Sac; Carbosynth Ltd., Compton, Berkshire, UK), mannitol (Pearlitol 100SD, Roquette, Lestrem, France), microcrystalline cellulose (MCC; Pharmacel 102, DFE Pharma, Goch, Germany), croscarmellose sodium (CCS; Ac-Di-Sol, FMC Biopolymer, Philadelphia, PA) and magnesium stearate (MgSt; Mallinckrodt Inc., St. Louis, MO) were used as received. Commercial Lor chewable tablets (Children's Claritin Chewable Tablet (loratadine 5 mg); Bayer Healthcare LLC., Whippany, NJ) were purchased from CVS Pharmacy (Minneapolis, MN).

3.2.2 Methods

3.2.2.1 Preparation of bulk Lor-Sac salt

Bulk powders of Lor-Sac salt were prepared by dissolving Lor (7.67 g, 0.02 mol) and Sac (3.66 g, 0.02 mol) in ethyl acetate at a 1:1 molar ratio under ambient condition. The solution was clear, colorless and sticky at first but large amount of solid precipitated out after continuous stirring. Crystals suitable for single crystal X-ray diffractometry

examination were prepared by re-dissolving small amount of bulk powder (2.5 mg) into 5 mL ethyl acetate followed by slow evaporation in a cold room (4℃).

3.2.2.2 Single Crystal X-ray Diffractometry

Single crystal X-ray diffraction (SCXRD) experiments were performed on a Bruker-AXS Venture Photon-II diffractometer (Bruker AXS Inc., Madison, Wisconsin) using MoKα radiation at 100 K. Intensity data were corrected for absorption and decay using SADABS. The crystal structure was solved and refined using ShelXle [25]. Direct methods were employed to locate most non-hydrogen atoms from the E-map. Full-matrix least-squares/difference Fourier cycles were performed to refine the position of non-hydrogen atoms. All non-hydrogen atoms were refined with anisotropic displacement parameters. Remaining hydrogen atoms were placed according to the residual peaks in the Fourier map.

3.2.2.3 Powder X-ray Diffractometry

Powder X-ray diffraction (PXRD) patterns were obtained from a wide-angle diffractometer (X'pert Pro; PANalytical, Westborough, MA) using Cu Kα radiation (45 kV and 40 mA, wavelength of 1.54059 Å.) at ambient temperature. Samples were scanned between 5 and 35° 2θ with a step size of 0.016° and a dwell time of 1s/step.

3.2.2.4 Fourier Transformation Infrared Spectroscopy (FT-IR)

FT-IR spectra of dry sample powders was obtained from a FT-IR spectrometer (Nicolet™ iS50, Thermo Scientific, Waltham, MA) equipped with a diamond attenuated total reflection (ATR) and DLaTGS detector. The average graph of each sample was taken after 32 scans in the range of 4000−450 cm^{-1} at a resolution of 2 cm^{-1}.

3.2.2.5 Thermal Analysis

Thermal stability was analyzed using thermogravimetric analysis (TGA) and differential scanning calorometry (DSC). For TGA, approximately 3 mg of each sample was placed in an open aluminum pan and heated on a thermogravimetric analyzer (Q500; TA Instruments, New Castle, DE) from room temperature to 250°C at 10°C/min under dry nitrogen purge (75 mL/min).

For DSC, Approximately 3 mg of sample was loaded into Tzero hermetically sealed aluminum pans and heated on a differential scanning calorimeter (Q1000, TA Instruments, New Castle, DE) from room temperature to 175 °C at a heating rate of 10 °C/min under a continuous nitrogen purge at a flow rate of 25 mL/min. DSC cell parameter was calibrated with indium for heat flow, indium and cyclohexane for temperature.

Both TGA and DSC data were analyzed using Universal Analysis 2000 software (TA Instruments, New Castle, DE).

3.2.2.6 Hot Stage Microscopy

Crystals were observed under a polarized light microscope (Eclipse e200; Nikon, Tokyo, Japan), while being heated to 175 °C on a hot stage (Linksys 32; V.2.2.0, Linkam Scientific Instruments, Ltd., Waterfield, UK) at a constant rate of 5 °C/min. Photos of crystals at different temperature were captured by a DS-Fi1 microscope digital camera.

3.2.2.7 Dynamic Vapor Sorption (DVS)

Water sorption isotherms were obtained using an automated vapor sorption analyzer (Intrinsic DVS, Surface Measurement Systems Ltd., Allentown, PA, USA) at 25 °C with nitrogen flow rate of 50 mL/min. Each sample was equilibrated at a specified relative humidity (RH), ranging from 0% to 95% in 5% increments in this work, and sample weight was monitored by a micro balance. Once one of two equilibration criteria, $dm/dt \leq 0.003\%$ or maximum equilibration time of 6 h, was reached, the RH was changed to the next target value by controlling flow rates of the dry and wet lines of nitrogen gas.

3.2.2.8 Solubility and Intrinsic Dissolution Rate (IDR)

The solubility of Lor and Lor-Sac was determined in a water-methanol medium (1:1 v/v) by suspending an excess amount of solid (100 mg) in 5 mL of the medium under stirring at 23℃ for 24 h. The sovlent mixture was used so that the solubility of Lor could be monitored by a UV (DU 530 UV/vis spectrophotometer; Beckman Coulter, Chaska, Minnesota). Otherwise, no detectable dissolution of Lor was observed by UV in water due to extremely low solubility. In addition, the PXRD patterns of residual solids were

collected to identify crystal form. Lor-Sac was found to convert into Lor when slurred for 24h in water (Fig. 3.2). The dissociation of Lor-Sac was avoided in the mixed solvent system (Fig. 3.2). The suspensions were filtered through 0.45 μm PTFE membrane filters. The filtrates were appropriately diluted with medium for measurement by a UV/vis spectrometer. Solution concentrations were determined from the absorbance based on a previously constructed calibration curve (Fig. 3.3). All measurements were performed in triplicate.

The intrinsic dissolution rate (IDR) of both Lor and Lor-Sac were determined using a modified rotating disc method[26]. Approximately 20 mg of powders were compressed at a force of 2000 lb in a custom-made steel die for 2 min to prepare a pellet (6.39 mm in diameter). The dissolution medium was the same as that for the solubility test. The die containing pellet was immersed and rotated at 300 rpm in 150 mL dissolution medium at 23°C, an UV-Vis fiber-optic probe (Ocean Optics, Dunedin, FL) was used to continuously monitor the UV absorbance of the solution. Solution concentrations were determined using the absorbance and from a previously constructed calibration curve (Fig. 3.4). IDR was calculated from the initial slope of the linear portion of the concentration - time profile and the pellet surface area exposed to the dissolution medium.

3.2.2.9 Formulation and Powder Compaction

The compositions of a chewable tablet formulation are summarized in Table 3.1. Each component in the formulation was first passed through a 250 μm sieve and mixed in

a glass bottle. The bottle was blended on a mixer (Turbula, Glen Mills Inc., Clifton, NJ) at 49 rpm for 2 min. 1% MgSt was added to the bottle and the whole formulation was further blended for 4 min.

A material testing machine (model 1485, Zwick/Roell, Ulm, Germany) was used to explore the optimal compaction pressure for this chewable tablet formulation. Tablets with approximately 250 mg of weight were prepared separately over the 25-300 MPa pressure range at a punch speed of 5 mm/min (9.5 mm flat faced punch). Tablets were relaxed under ambient conditions for at least 24 h before measuring their dimensions and diametrical breaking force.

Tablet diametrical breaking force was determined using a texture analyzer (TA-XT2i; Texture Technologies Corporation, Scarsdale, NY) at a speed of 0.01 mm/s with a 5 g trigger force. Tablet tensile strength was calculated from Eq. (3.1) [27]:

$$\sigma = \frac{2F}{\pi D h} \tag{3.1}$$

where F, D, and h are the breaking force (N), tablet diameter (mm), and thickness (mm), respectively.

After determining the optimal compaction pressure, a compaction simulator (Presster, Metropolitan Computing Company, East Hanover, NJ) was used to simulate a 29-station Korsch XL400 high-speed tablet press (9.5 mm flat faced punch). The dwell time was set at 20 ms, corresponding to a linear speed of 0.423 m/s (52,000 tablets/h).

Chewing difficulty index (CDI), proposed by Food and Drug Administration (FDA), a was calculated from Eq. (3.2) to quantify the level of difficulty in chewing a tablet [28]:

$$CDI = F_d \cdot h \quad (3.2)$$

where F_d and h are the diametrical breaking force and tablet thickness, respectively. The unit of CDI is N·m.

3.2.2.10 Powder Flowability

Flowability of the chewable tablet formulation was measured using a ring shear cell tester (RST-XS; Dietmar Schulze, Wolfenbüttel, Germany). A cell with 10 mL volume was used for collecting data at the preshear normal stresss of 1 kPa and the measurements were triplicated, from which flowability index (*ff*c) was calculated to quantify powder flowability[29].

3.2.2.11 Expedited Friability

Tablet friability profile of the chewable tablet formulation was obtained using an expedited method[30]. Tablets compressed under different compaction pressures were coded and tested in a friabilator (Model F2, Pharma Alliance Group Inc., Santa Clarita, CA) running at 25 rpm for 4 minutes. The percentage weight loss was calculated for each tablet and plotted against compaction pressure.

3.3 Results and discussion

3.3.1 Crystal structure analysis

The Lor-Sac crystallized in the monoclinic space group $P2_1/c$ with Z'=1 (detailed crystallographic information in Table 3.2). The asymmetric unit contains Lor and Sac in 1:1 molar ratio (Fig. 3.5a). There are four asymmetric units in the unit cell (Z = 4, Fig. 3.5b). The proton transfer from amide group of Sac to the pyridine nitrogen of Lor indicates the formation of a salt.[31, 32] The Lor^+ and Sac^- are assembled *via* charge assisted N^+-H···N^- ($d_{D\ldots A}$: 2.670 Å, 172.25°) hydrogen bond. The hydrogen bond length and angle are comparable to those from reported salts that contain N^+-H···N^- bond formed by Sac^-. [33, 34] The Lor^+ and Sac^- pairs are connected through S=O···H-C (3.101 and 3.264 Å), C-H···O (3.231 Å) hydrogen bonds along the *bc* plane (Fig. 3.5c) to form a 2D layered structure. Only weak S=O···H-C (3.394 Å), C-H···Cl (3.367 Å) and C-H···O (3.361 Å) hydrogen bonds (Fig. 3.5d) were observed between adjacent layers.

3.3.2 Solid state characterization

The phase purity of bulk powders prepared by slurry method was confirmed as all peaks in PXRD patterns matched well with those calculated from the single crystal structure (Fig. 3.6). Compared to Lor and Sac, the characteristic peaks of Lor-Sac are at 11.76, 14.74, 18.16 and 21.64°. The absence of characteristic peaks of Lor and Sac also supports their complete conversion to salt in the prepared bulk salt powder.

In the FT-IR spectra of Lor-Sac, characteristic peaks of both Lor and Sac could be observed in Lor-Sac (Fig. 3.7). For example, the C-O stretching peak at 1275cm^{-1} from the ester chain of Lor and the S=O stretching peaks at 1330cm^{-1}, 1170cm^{-1} from the sulfonamide group of Sac are visible. The shift of of N-H (3100cm^{-1}) and C=O (1700cm^{-1}) stretching peaks indicates their participation in different hydrogen bonds.

The melting point of Lor-Sac (140.95℃) is in between those of Lor (135℃) and Sac (228℃) (Fig. 3.8a). The TGA profile (Fig. 3.8b) showed no weight loss before melting point, suggesting neither decomposition nor sublimation occurred before the salt melted. In addition to stability against high temperature, Lor-Sac is also stable against high RH. Isothermal moisture sorption analysis showed less than 1.0% weight gain up to 95% RH (Fig. 3.9). The higher moisture absorption of Lor-Sac than Lor suggests potential wettability and solubility improvement of Lor-Sac over Lor [35, 36].

Overall data suggest that Lor-Sac is physically stable under typical pharmaceutical manufacturing and storage conditions. Thus, Lor-Sac is an acceptable candidate for further tablet product development.

3.3.3 Solubility and intrinsic dissolution rate

Enhancement of solubility and dissolution rate is one of the potential pharmaceutical advantages of salts. The solubility and intrinsic dissolution rate data are summarized in Table 3.3 (see Fig. 3.10 for IDR profiles).

Both solubility (×9.8) and dissolution rate (×11) of Lor-Sac were significantly higher than those of pure Lor. The linearity of IDR profiles of Lor-Sac indicates an absence of disproportionation in the water-methanol mixture during the time frame of IDR experiments. If salt disproportionation can be inhibited, for examples by using appropriate precipitation inhibitors[37], the same dissolution advantage of Lor-Sac can be expected in water. The higher solubility of Lor-Sac may be attributed to the highly hydrophilic Sac^-, which facilitates the release of Lor[38, 39]. In addition, the hydrophobic ester chain of Lor is buried under the surface of the crystal while the hydrophilic Sac is exposed to the surface of Lor-Sac crystals[40, 41].

3.3.4 Chewable tablet formulation design

Lor-Sac exhibited better pharmaceutical properties over Lor, especially the solubility at physiological pHs and sweet taste[23, 26]. These advantages make it a good candidate for chewable tablet development.

A good chewable tablet must meet several criteria: (1) appropriate hardness (easy to chew but still can withstand normal handling), (2) palatable (comfortable taste and mouth feel), (3) suitable size and shape, and (4) easy disintegration (facilitate dissolution and avoid side effect like gastrointestinal obstruction)[42].

With these criteria in mind, we proposed a chewable tablet formulation as summarized in Table 3.1. Mannitol was chosen as the filler of this chewable tablet

formulation because of its low hygroscopicity, inertness towards active pharmaceutical integrant (API) and acceptable tableting behavior[43]. Among all of the commercially available grades of mannitol, the intermediate tensile strength and excellent flowability made mannitol 100SD the best choice for this chewable tablet formulation[44, 45]. Additionally, mannitol 100SD particles, d50 ~125 μm, are much smaller than 250 μm, which eliminates the possible problem of grittiness [46]. A small amount of MCC was added to improve the tablet mechanical strength. The super-disintegrant CCS in formulation functions to reduce tablet size when contacting with saliva in oral cavity to avoid unwanted obstruction in digestive tract. It is noteworthy to mention that no additional sweetener is included in this formulation since the counterion, Sac^-, is a potent artificial sweetener (300 times as sweet as sucrose)[47] and the amount of Sac in Lor-Sac is sufficient to enable the palatability of the chewable tablet.

3.3.5 Determination of optimal compaction pressure

A successful tablet formulation should have both good flowability and tabletability. Adequate flowability assures consistent die filling and uniform tablet weight, while good tabletability allows the preparation of tablets with sufficient mechanical strength to sustain handling and storage processes after compression. The flowability of the proposed Lor chewable tablet formulation is much higher (ff_c = 11 at 1kPa) than that of Avicel PH102 (ff_c = 6 at 1kPa), largely due to the excellent flowability of the grade of mannitol used in

the formulation. Therefore, flowability is not an issue for this formulation even for a high-speed tableting process[48].

Tabletability is the capacity of a powder to be transformed into a tablet of specified strength under the effect of compaction pressure, which is usually presented by a plot of tensile strength against compaction pressure[49, 50]. For the proposed Lor chewable tablet formulation, tensile strength increased linearly with increasing compaction pressure ($R^2 >$ 0.99, Fig. 3.11). The tensile strength is > 1.28 MPa, the average tensile strength of commercial Lor chewable tablets (Children's Claritin Chewable Tablet) (n = 6, Table 3.4), at 100 MPa compaction pressure or higher.

Although lower tablet strength favors easier chewing, very weak tablets exhibit very high friability are not commercially viable. An ideal chewable tablet should be strong enough to avoid the friability problem but not too strong to present difficulty with chewing. Therefore, the acceptable design space of a chewable tablet is defined by friability, tablet variability, and chewing difficulty index (CDI).

Tablet friability is the tendency of a tablet to lose component particles due to wear and tear during manufacturing, storage, and handling. Friability plots, percentage weight loss as a function of compaction pressure, is a very useful way to characterize friability of a formulation[30, 51]. The percentage weight loss of Lor chewable tablets prepared at different pressures followed a power law relationship (Fig. 3.12), as observed in other materials[52, 53]. From this profile, the compaction pressure corresponding to 1.0% friability

is approximately 100 MPa. Therefore, compaction pressure should be at least 100 MPa to avoid excessive friability. Combining tabletability and friability data, any pressures higher than 100 MPa is suitable for manufacturing chewable tablets with sufficient mechanical strength for this formulation.

CDI has been proposed to evaluate difficulty to chew a tablet[28, 42]. Calculating CDI only requires tablet diametrical breaking force and thickness. CDI appropriately accounts for the effect of tablet thickness on chewability since a thinner tablet is easier to chew when hardness is the same. In absence of a universal CDI criterion, CDI of a commercial chewable tablet product was measured as a reference (Fig. 3.13), which exhibited CDI in the range of 0.175 - 0.2 Nm. The 0.2 CDI corresponds to a compaction pressure of 125 MPa for the proposed chewable formulation. Thus, any pressure between 100 and 125 MPa can be used to manufacture tablets with both low friability and acceptable chewability. This compaction pressure range was further evaluated at a high speed using a compaction simulator with a dwell time of 20 ms (corresponding to 52,000 tablets/h). At 100 MPa, tablet tensile strength was 1.55 ± 0.02 MPa (n = 6), the CDI was 0.182 ± 0.003 N·m (n = 6), and tablet weight variation was 0.06% (249.2 ± 0.17 mg, n = 6). This is better than the reference commercial chewable tablet, with tensile strength of 1.28 ± 0.06 MPa (n = 6), CDI of 0.188 ± 0.009 N·m (n = 6) and tablet weight variation of 0.9% (247.0 ± 2.22 mg, n = 6). Therefore, chewable Lor tablets can be manufactured under commercial tableting conditions using the proposed Lor tablet formulation in Table 3.1.

3.4 Conclusion

We have prepared and characterized a novel salt of Lor with Sac. This sweet salt exhibits enhanced solubility and dissolution rate. A chewable tablet formulation based on Lor-Sac was successfully designed. The new chewable tablet of Lor achieved acceptable pharmaceutical properties without the risk of physical segregation between drug and sweetener encountered in conventional chewable tablet formulations. This is another example of expedited development of a challenging tablet dosage form enabled by crystal engineering.

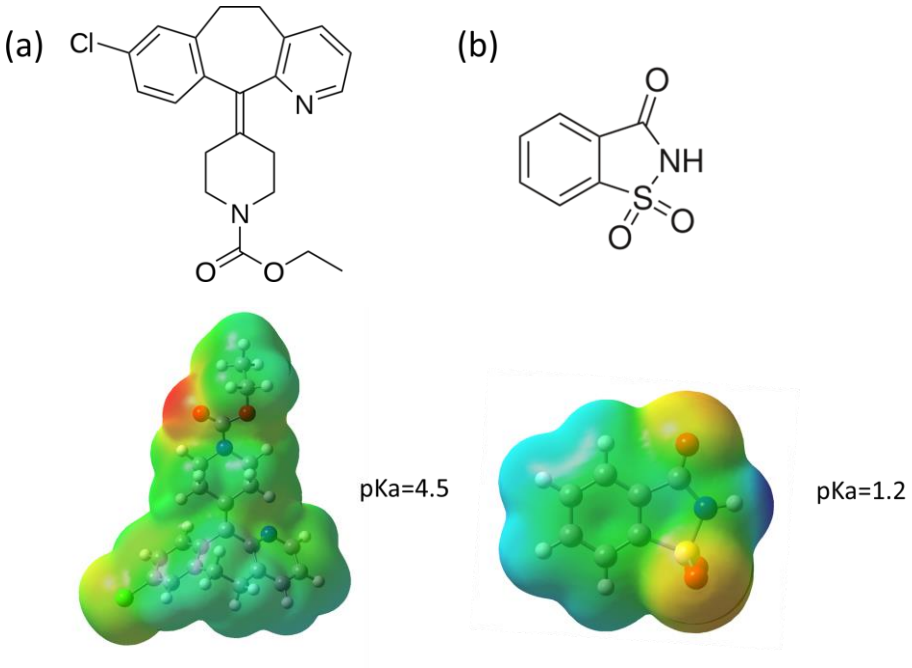

Figure 3.1 Molecular structures and electrostatic potentials maps of (a) loratadine (MW = 382.88 g/mol, pK_a = 4.5) and (b) saccharin (MW = 183.18 g/mol, pK_a = 1.2).

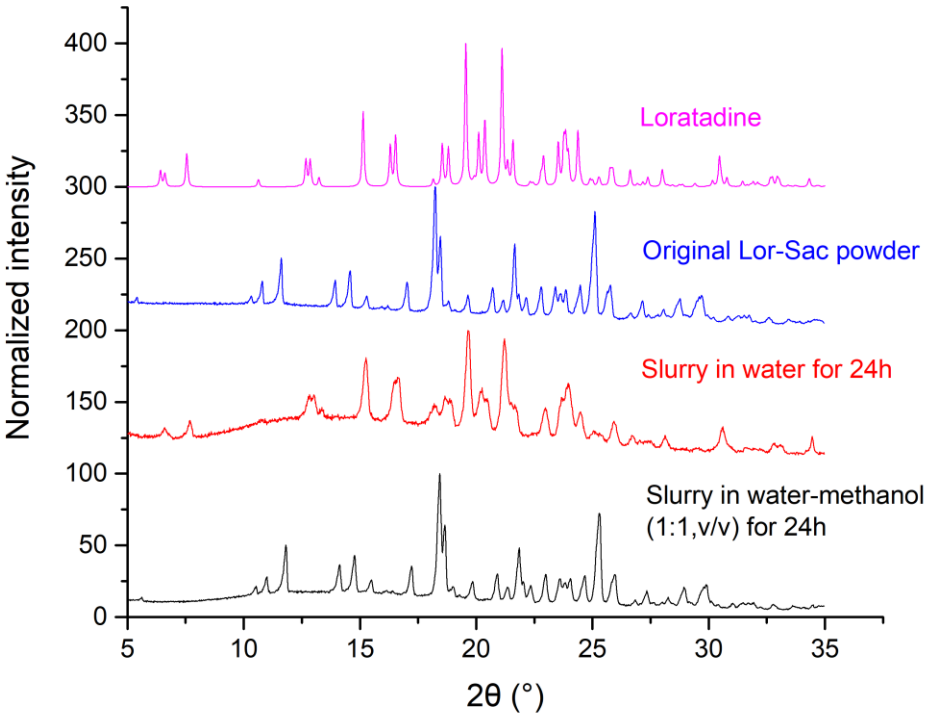

Figure 3.2 PXRD patterns of Lor-Sac after solubility test

(a)

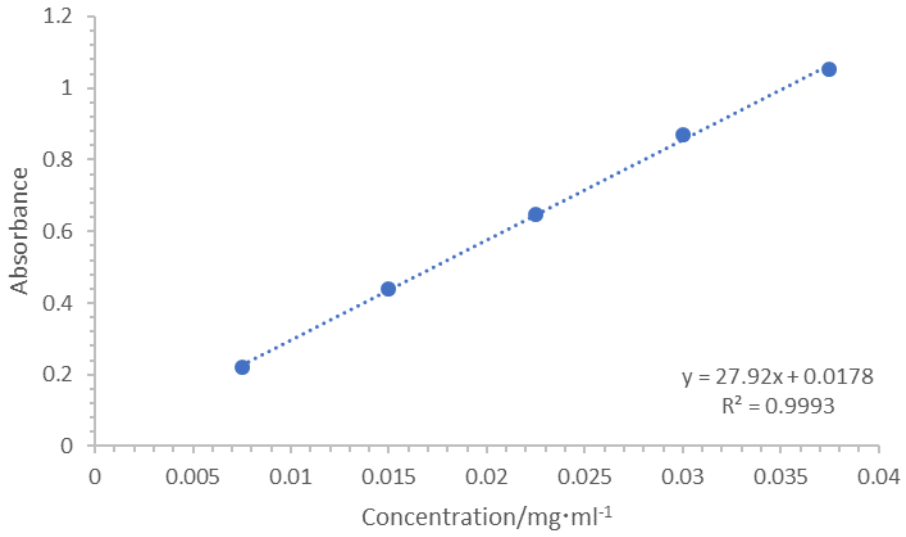

(b)

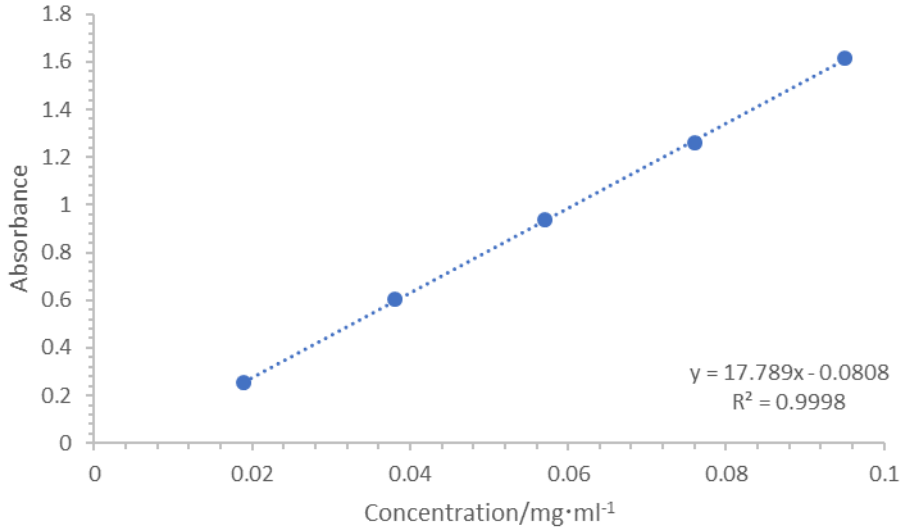

Figure 3.3 Calibration curve of (a) Lor and (b) Lor-Sac for the determination of solubility. Equipment: UV/vis spectrometer (DU530 UV/vis spectrophotometer; Beckman Coulter, Chaska, MN); Detection wavelength: 247nm for Lor, 270nm for Lor-Sac.

(a)

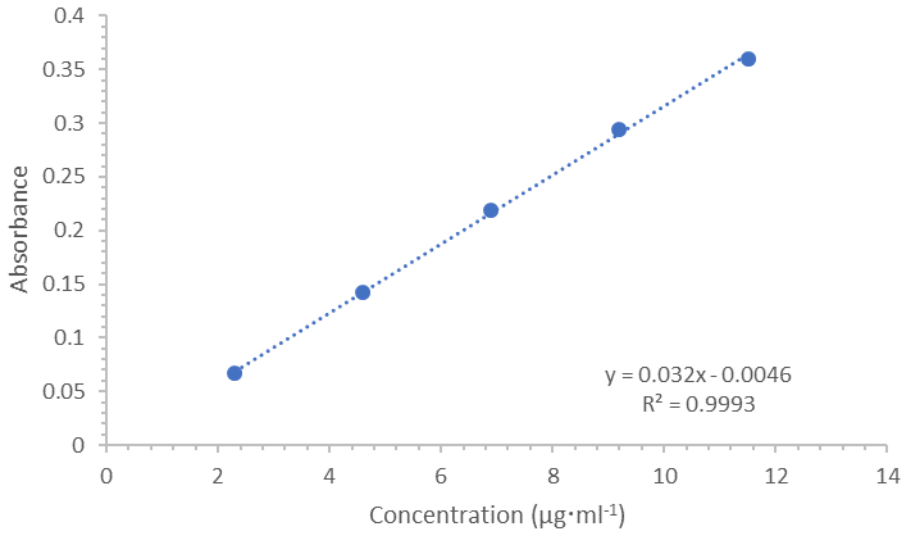

(b)

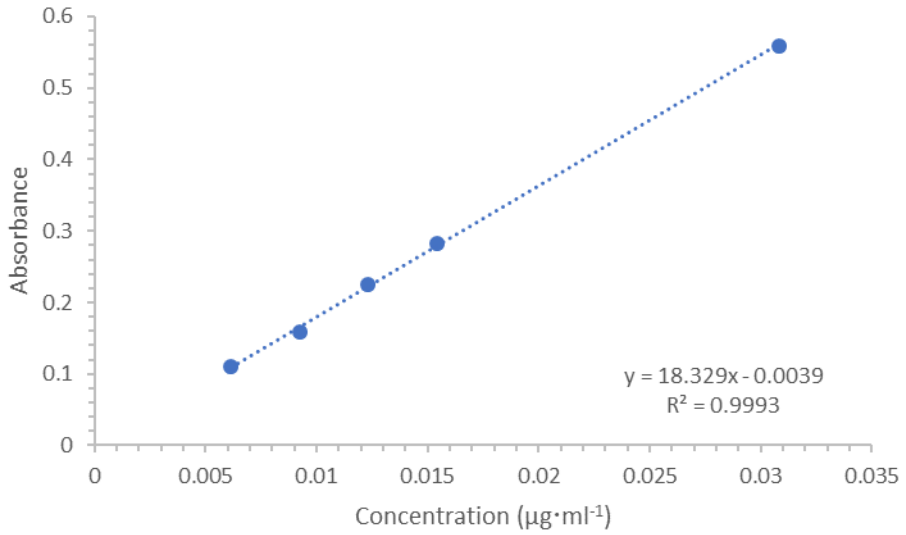

Figure 3.4 Calibration curve of (a)Lor and (b)Lor-Sac for the UV-Vis fiber-optic probe (IDR). Equipment: UV-Vis fiber-optic probe (Ocean Optics, Dunedin, FL); Detection wavelength: 247nm for Lor, 270nm for Lor-Sac.

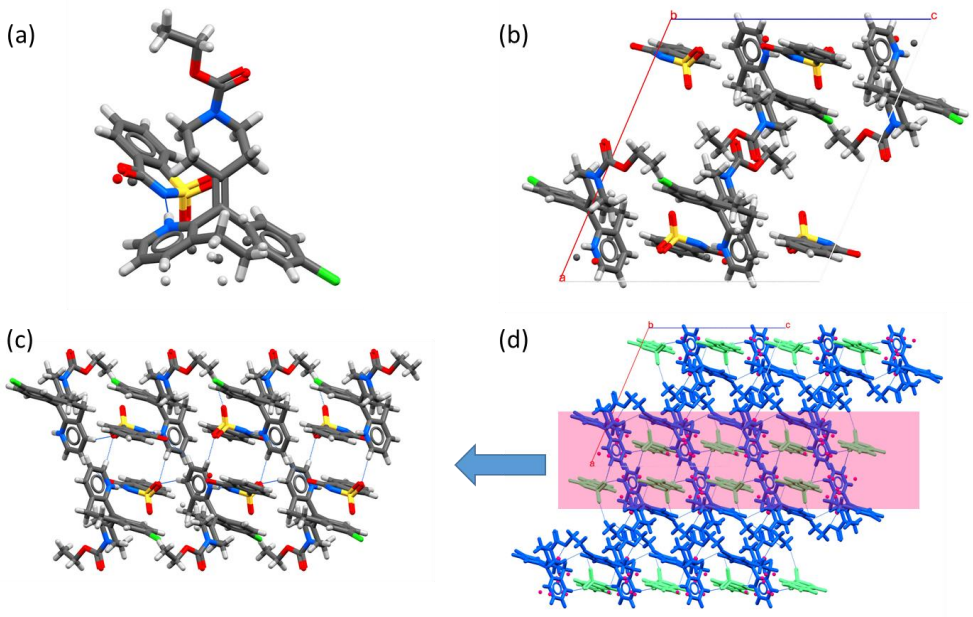

Figure 3.5 Crystal structure of Lor-Sac: (a) asymmetric unit, (b) unit cell, (c) 2D layer structure, and (d) 3D packing pattern.

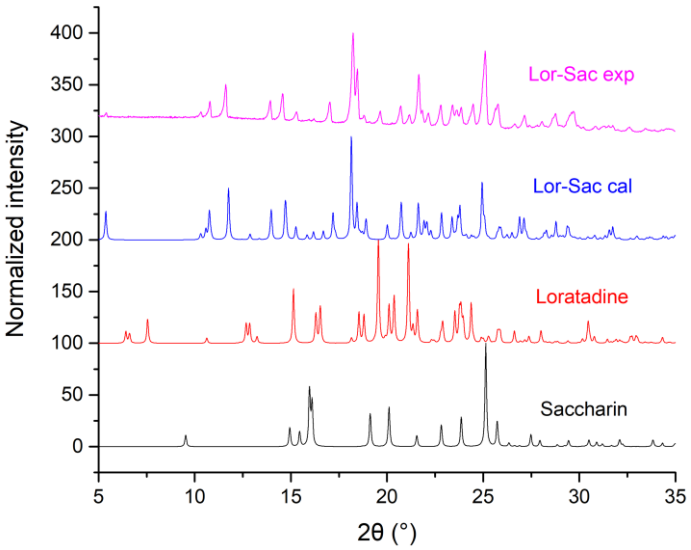

Figure 3.6 Powder X-ray diffraction patterns of Lor, Sac, and Lor-Sac (both experimental and calculated).

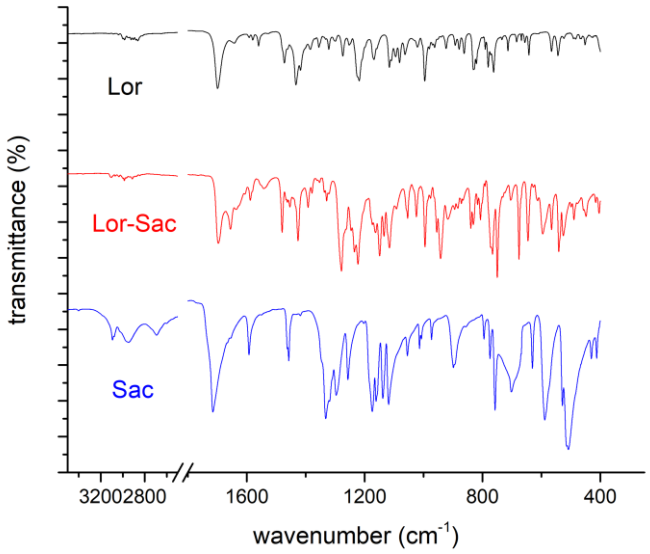

Figure 3.7 FT-IR spectra of Lor, Sac, and Lor-Sac

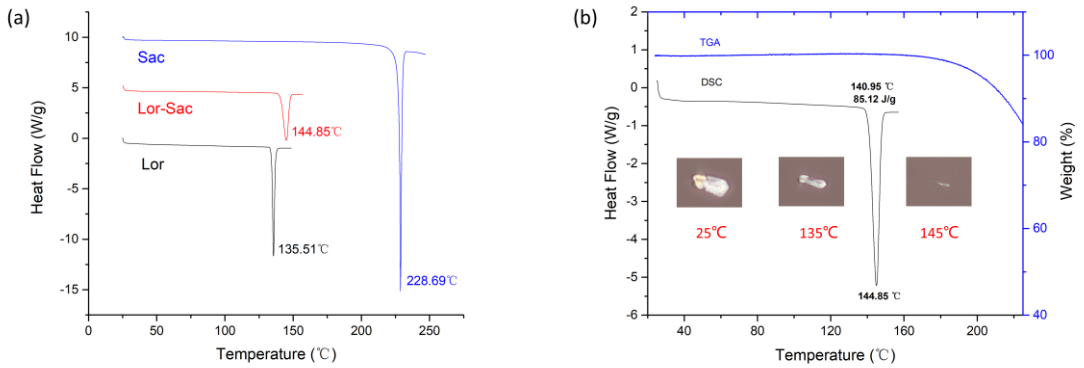

Figure 3.8 Thermal behavior of Lor-Sac characterized by (a) differential scanning calorimetry, (b) thermogravimetric analysis, and hot stage microscopy.

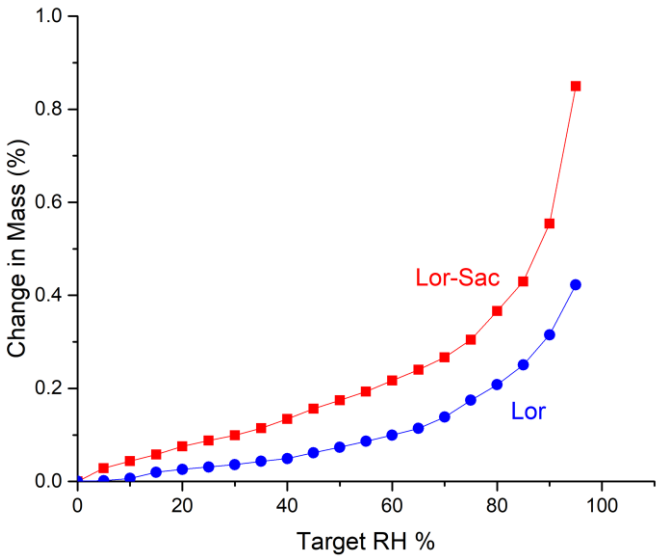

Figure 3.9 Moisture sorption behavior of Lor-Sac and Lor

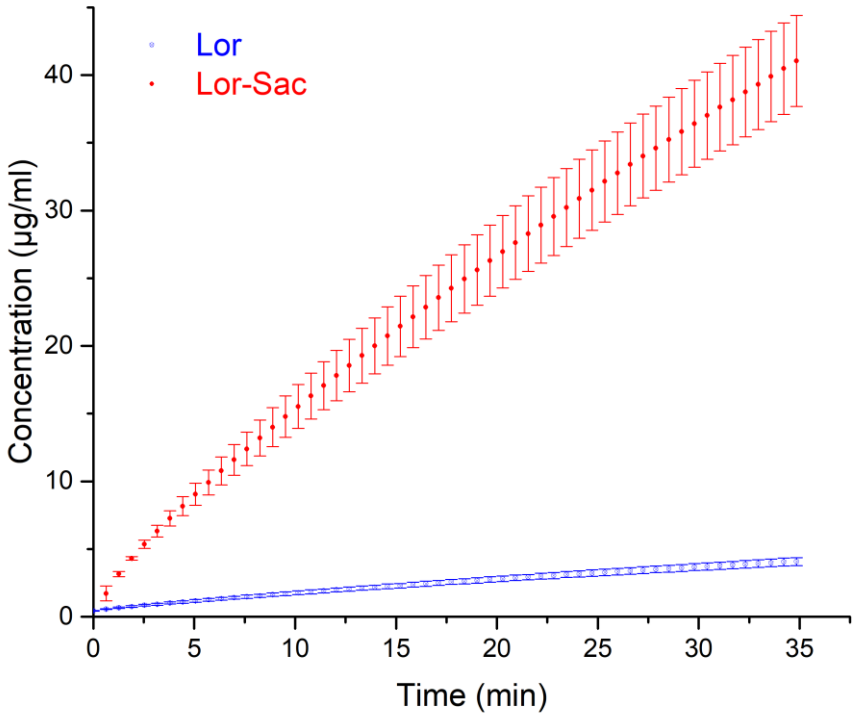

Figure 3.10 Intrinsic dissolution rate profile of Lor and Lor-Sac

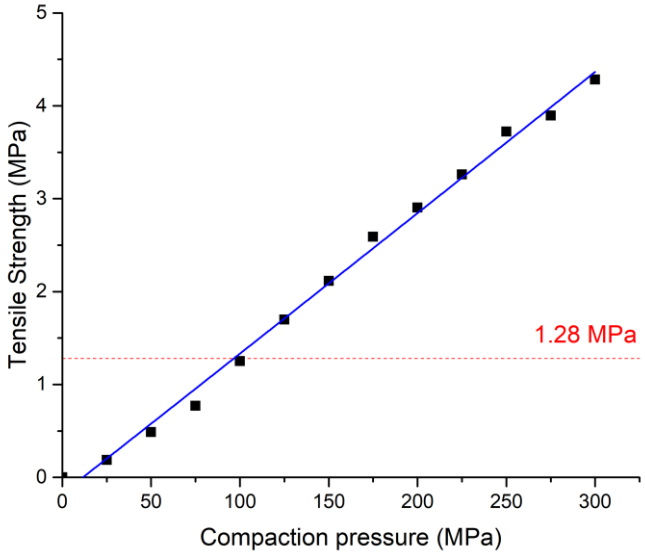

Figure 3.11 Tabletability profile of the chewable tablet formulation. The dashed horizontal line marks the average tensile strength of commercial Lor chewable tablets (Children's Claritin Chewable Tablet).

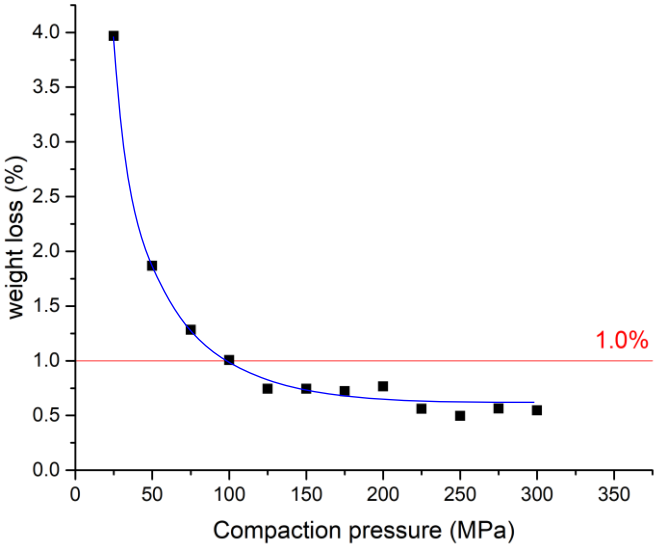

Figure 3.12 Friability profile of the chewable tablet formulation. Red line indicates the friability acceptance limit of 1% weight loss.

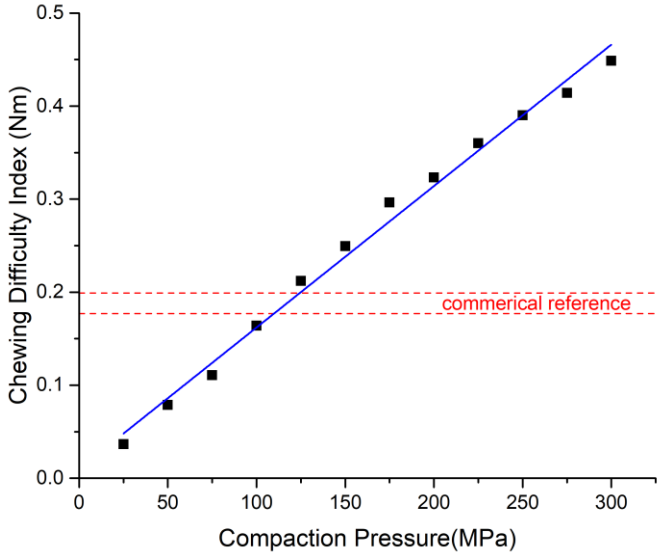

Figure 3.13 CDI of the proposed chewable tablet formulation. 95% confidence interval of the CDI of a batch of commercial chewable tablets is marked by the two horizontal lines (n=6)

Table 3.1 Chewable tablet formulation

Material	**Amount (w/w)**
Loratadine-Saccharin (Lor-Sac)	3.75%
Mannitol	82.25%
MCC	8.0%
CCS	5.0%
MgSt	1.0%

Table 3.2 Crystallographic information of loratadine-saccharin salt

Loratadine-Saccharin Salt	
Formula	$C_{29}H_{28}ClN_3O_5S$
Formula weight	566.06
Crystal system	Monoclinic
Space group	P 21/c
a, Å	17.8526(18)
b, Å	10.0517(11)
c, Å	16.3428(15)
β, °	113.069(4)
Volume, $Å^3$	2698.18
Z	4
Z’	1
T, K	100
R-factor	4.37
Density, g/cm^3	1.393

Table. 3.3 Intrinsic dissolution rate and solubility of Lor and Lor-Sac in MeOH-H_2O (1:1, v/v) at 23℃) (n=3)

Solid form	Solubility ($mg \cdot ml^{-1}$) [a]	IDR ($\mu g \cdot cm^{-2} \cdot s^{-1}$) [a]
Lor	1.583±0.073	28.92±1.65
Lor-Sac	15.52±0.48	322.22±22.31

Table 3.4 Summary of chewable tablet parameters of commercial reference

No.	Tablet thickness (mm)	Tablet diameter (mm)	Breaking force (N)	Tensile strength (MPa)	CDI (Nm)
1	3.16	9.55	61.44	1.30	0.194
2	3.14	9.54	60.01	1.28	0.188
3	3.15	9.54	64.92	1.38	0.204
4	3.12	9.55	58.71	1.25	0.183
5	3.14	9.56	57.81	1.23	0.182
6	3.11	9.55	57.26	1.23	0.178
Average				1.28	0.188
SD				0.06	0.010

CHAPTER 4 Research summary and Future work

4.1 Research Summary

The research based on two classic antihistamines-loratadine and desloratadine successfully demonstrated how to utilize pharmaceutical materials science and tools to understand compaction behavior of bulk drug powder and improve physical properties and manufacturability of drug product.

Chapter 2

In Chapter 2, the origin of different mechanical properties and tableting behavior between Lor and Des were systematically investigated. The significantly higher tabletability of Lor bulk powder than that of Des is attributed to its both larger bonding area and higher bonding strength. The larger bonding area of Lor is originated from its higher plasticity, which is confirmed computationally by energy framework calculation and topology analysis. The greater bonding strength of Lor is attributed to its much larger intermolecular dispersive interaction than Des. This study reveals new insights into the molecular origin of bonding area and bonding strength that is critical for understanding tabletability.

Chapter 3

In Chapter 3, we have prepared and characterized a novel salt of Lor with Sac. This sweet salt exhibits enhanced solubility and dissolution rate. A chewable tablet formulation based on Lor-Sac was successfully designed. The new chewable tablet of Lor is easy and less expensive to manufacture, while achieving better pharmaceutical

properties without the risk of physical segregation between drug and sweetener in conventional chewable tablet formulations. This is a good example of expedited development of a challenging tablet dosage form enabled by crystal engineering.

4.2 Future work

In Chapter 2, we provided molecular insight into bonding area and bonding strength. The dispersive surface energy was correlated to bonding strength for the first time. The reliability of this promising correlation should be evaluated in different molecular systems.

In Chapter 3, we synthesized a new salt of Lor and developed a chewable tablet formulation using it. Other artificial sweeteners, including acesulfame and aspartame, may also be suitable to modify drugs with poor pharmaceutical properties. The effectiveness of different sweeteners should be systematically evaluated and compared to guide future selection following the crystal engineering approach described in this work. Chewing difficulty index is an empirical parameter. More research is needed to further develop it or even develop a new index to assess the chewing difficulty of tablet. For the chewable formulation developed in this research, further evaluations, such as stability and dissolution, are required to ensure its commercial success.

Bibliography

Chapter 1

1. Huang, L.-F.; Tong, W.-Q. Impact of solid state properties on developability assessment of drug candidates. *Advanced Drug Delivery Reviews* **2004,** *56*, (3), 321-334.
2. Sun, C. C. Materials Science Tetrahedron—A Useful Tool for Pharmaceutical Research and Development. *Journal of Pharmaceutical Sciences* **2009,** *98*, (5), 1671-1687.
3. Joiris, E.; Martino, P. D.; Berneron, C.; Guyot-Hermann, A.-M.; Guyot, J.-C. Compression Behavior of Orthorhombic Paracetamol. *Pharmaceutical Research* **1998,** *15*, (7), 1122-1130.
4. Tye, C. K.; Sun, C.; Amidon, G. E. Evaluation of the effects of tableting speed on the relationships between compaction pressure, tablet tensile strength, and tablet solid fraction. *Journal of Pharmaceutical Sciences* **2005,** *94*, (3), 465-472.
5. Rohrs, B. R.; Amidon, G. E.; Meury, R. H.; Secreast, P. J.; King, H. M.; Skoug, C. J. Particle Size Limits to Meet USP Content Uniformity Criteria for Tablets and Capsules. *Journal of Pharmaceutical Sciences* **2006,** *95*, (5), 1049-1059.
6. Yu, L. X.; Amidon, G.; Khan, M. A.; Hoag, S. W.; Polli, J.; Raju, G. K.; Woodcock, J. Understanding pharmaceutical quality by design. *The AAPS journal* **2014,** *16*, (4), 771-783.
7. Simons, F. E.; Simons, K. J. Histamine and H1-antihistamines: celebrating a century of progress. *J. Allergy. Clin. Immunol.* **2011,** *128*, (6), 1139-1150.e4.
8. Waller, D. G.; Sampson, A. P., 39 - Antihistamines and allergic disease. In *Medical Pharmacology and Therapeutics (Fifth Edition)*, Fifth Edition ed.; Waller, D. G.; Sampson, A. P., Eds. Elsevier: 2018; pp 451-456.
9. Slater, J. W.; Zechnich, A. D.; Haxby, D. G. Second-Generation Antihistamines. *Drugs* **1999,** *57*, (1), 31-47.
10. Simons, F. E. Advances in H1-antihistamines. *N. Engl. J. Med.* **2004,** *351*, (21), 2203-17.
11. Nolen, T. M. Sedative effects of antihistamines: safety, performance, learning, and quality of life. *Clinical Therapeutics* **1997,** *19*, (1), 39-55.
12. Vilani Frank, J. Antihistaminic 11-(4-piperidylidene)-5h-benzo-[5,6]-cyclohepta-[1,2-b]-pyridines. US 4282233 A, 1980/06/19, 1981.
13. Timmerman, H., Histamine H1 Blockers: From Relative Failures to Blockbusters within Series of Analogues. In *Analogue-based Drug Discovery*, Fischer, J.; Ganellin, C. R., Eds. 2006.
14. Lieberman, P.; Hernandez-Trujillo, V.; Lieberman, J.; Frew, A. J., 89 - Antihistamines. In *Clinical Immunology (Third Edition)*, Rich, R. R.; Fleisher, T. A.; Shearer, W. T.; Schroeder, H. W.; Frew, A. J.; Weyand, C. M., Eds. Mosby: Edinburgh, 2008; pp 1317-1329.

15. Hilbert, J.; Radwanski, E.; Weglein, R.; Luc, V.; Perentesis, G.; Symchowicz, S.; Zampaglione, N. Pharmacokinetics and Dose Proportionality of Loratadine. *The Journal of Clinical Pharmacology* **1987,** *27*, (9), 694-698.
16. Kreutner, W.; Hey, J. A.; Anthes, J.; Barnett, A.; Young, S.; Tozzi, S. Preclinical Pharmacology of Desloratadine, a Selective and Nonsedating Histamine H1 Receptor Antagonist. *Arzneimittelforschung* **2000,** *50*, (04), 345-352.
17. Radwanski, E.; Hilbert, J.; Symchowicz, S.; Zampaglione, N. Loratadine: Multiple-Dose Pharmacokinetics. *The Journal of Clinical Pharmacology* **1987,** *27*, (7), 530-533.
18. Clark, M. J.; Million, R. P. Allergic rhinitis: market evolution. *Nat. Rev. Drug Discov.* **2009,** *8*, (4), 271-2.
19. Trygstad, T. K.; Hansen, R. A.; Wegner, S. E. Evaluation of product switching after a state Medicaid program began covering loratadine OTC 1 year after market availability. *J. Manag. Care Pharm.* **2006,** *12*, (2), 108-20.
20. Villani, F. J. 8-Chloro-6,11-dihydro-11-(4-piperidylidene)-5H-benzo[5,6]cyclohepta-[1,2-b]pyridine and its salts, processes for the production thereof and pharmaceutical compositions containing these compounds. EP 0152897, 1984/02/15, 1984.
21. Affrime, M.; Gupta, S.; Banfield, C.; Cohen, A. A Pharmacokinetic Profile of Desloratadine in Healthy Adults, Including Elderly. *Clinical Pharmacokinetics* **2002,** *41*, (1), 13-19.
22. Geha, R. S.; Meltzer, E. O. Desloratadine: A new, nonsedating, oral antihistamine. *J. Allergy Clin. Immunol.* **2001,** *107*, (4), 751-62.
23. Molimard, M.; Diquet, B.; Benedetti, M. S. Comparison of pharmacokinetics and metabolism of desloratadine, fexofenadine, levocetirizine and mizolastine in humans. *Fundam. Clin. Pharmacol.* **2004,** *18*, (4), 399-411.
24. Ramanathan, R.; Reyderman, L.; Su, A. D.; Alvarez, N.; Chowdhury, S. K.; Alton, K. B.; Wirth, M. A.; Clement, R. P.; Statkevich, P.; Patrick, J. E. Disposition of desloratadine in healthy volunteers. *Xenobiotica* **2007,** *37*, (7), 770-87.
25. Jivraj, M.; Martini, L. G.; Thomson, C. M. An overview of the different excipients useful for the direct compression of tablets. *Pharmaceutical Science & Technology Today* **2000,** *3*, (2), 58-63.
26. Sun, C. C. Decoding Powder Tabletability: Roles of Particle Adhesion and Plasticity. *Journal of Adhesion Science and Technology* **2011,** *25*, (4-5), 483-499.
27. Davies, P., Oral solid dosage forms. In *Pharmaceutical preformulation and formulation*, CRC Press: 2015; pp 391-470.
28. Sun, C. C. Microstructure of Tablet—Pharmaceutical Significance, Assessment, and Engineering. *Pharmaceutical Research* **2017,** *34*, (5), 918-928.
29. Wang, C.; Paul, S.; Wang, K.; Hu, S.; Sun, C. C. Relationships among Crystal Structures, Mechanical Properties, and Tableting Performance Probed Using Four Salts of Diphenhydramine. *Cryst. Growth Des.* **2017,** *17*, (11), 6030-6040.
30. Chowhan, Z. T.; Yang, I. C.; Amaro, A. A.; Chi, L.-H. Effect of Moisture and Crushing Strength on Tablet Friability and In Vitro Dissolution. *Journal of Pharmaceutical*

Sciences **1982,** *71*, (12), 1371-1375.
31. Cooper, J.; Rees, J. E. Tableting Research and Technology. *Journal of Pharmaceutical Sciences* **1972,** *61*, (10), 1511-1555.
32. Sun, C.; Grant, D. J. W. Influence of Crystal Structure on the Tableting Properties of Sulfamerazine Polymorphs. *Pharmaceutical Research* **2001,** *18*, (3), 274-280.
33. Sun, C.; Grant, D. J. W. Effects of initial particle size on the tableting properties of l-lysine monohydrochloride dihydrate powder. *International Journal of Pharmaceutics* **2001,** *215*, (1), 221-228.
34. Bag, P. P.; Chen, M.; Sun, C. C.; Reddy, C. M. Direct correlation among crystal structure, mechanical behaviour and tabletability in a trimorphic molecular compound. *CrystEngComm* **2012,** *14*, (11), 3865-3867.
35. Krishna, G. R.; Shi, L.; Bag, P. P.; Sun, C. C.; Reddy, C. M. Correlation Among Crystal Structure, Mechanical Behavior, and Tabletability in the Co-Crystals of Vanillin Isomers. *Crystal Growth & Design* **2015,** *15*, (4), 1827-1832.
36. Sun, C.; Himmelspach, M. W. Reduced tabletability of roller compacted granules as a result of granule size enlargement. *Journal of Pharmaceutical Sciences* **2006,** *95*, (1), 200-206.
37. Narayan, P.; Hancock, B. C. The relationship between the particle properties, mechanical behavior, and surface roughness of some pharmaceutical excipient compacts. *Materials Science and Engineering: A* **2003,** *355*, (1), 24-36.
38. Sun, C. C. A material-sparing method for simultaneous determination of true density and powder compaction properties—Aspartame as an example. *International Journal of Pharmaceutics* **2006,** *326*, (1), 94-99.
39. Çelik, M., *Pharmaceutical Powder Compaction Technology*. CRC Press: 2016.
40. Sun, C. C.; Kiang, Y.-H. On the identification of slip planes in organic crystals based on attachment energy calculation. *Journal of Pharmaceutical Sciences* **2008,** *97*, (8), 3456-3461.
41. Wang, C.; Sun, C. C. Identifying Slip Planes in Organic Polymorphs by Combined Energy Framework Calculations and Topology Analysis. *Crystal Growth & Design* **2018,** *18*, (3), 1909-1916.
42. York, P. Crystal Engineering and Particle Design for the Powder Compaction Process. *Drug Development and Industrial Pharmacy* **1992,** *18*, (6-7), 677-721.
43. Desiraju, G. R., *Crystal Engineering: The Design of Organic Solids*. Elsevier: 1989.
44. Nangia, A. K.; Desiraju, G. R. Crystal Engineering: An Outlook for the Future. *Angewandte Chemie International Edition* **2019,** *58*, (13), 4100-4107.
45. Steed, J. W. The role of co-crystals in pharmaceutical design. *Trends Pharmacol. Sci.* **2013,** *34*, (3), 185-193.
46. Blagden, N.; de Matas, M.; Gavan, P. T.; York, P. Crystal engineering of active pharmaceutical ingredients to improve solubility and dissolution rates. *Adv. Drug Deliv. Rev.* **2007,** *59*, (7), 617-30.
47. Schultheiss, N.; Newman, A. Pharmaceutical Cocrystals and Their Physicochemical

Properties. *Cryst Growth Des* **2009,** *9*, (6), 2950-2967.
48. Duggirala, N. K.; Perry, M. L.; Almarsson, O.; Zaworotko, M. J. Pharmaceutical cocrystals: along the path to improved medicines. *Chem Commun (Camb)* **2016,** *52*, (4), 640-55.
49. Feng, L.; Karpinski, P. H.; Sutton, P.; Liu, Y.; Hook, D. F.; Hu, B.; Blacklock, T. J.; Fanwick, P. E.; Prashad, M.; Godtfredsen, S.; Ziltener, C. LCZ696: a dual-acting sodium supramolecular complex. *Tetrahedron Letters* **2012,** *53*, (3), 275-276.
50. Desai, A. S.; McMurray, J. J. V.; Packer, M.; Swedberg, K.; Rouleau, J. L.; Chen, F.; Gong, J.; Rizkala, A. R.; Brahimi, A.; Claggett, B.; Finn, P. V.; Hartley, L. H.; Liu, J.; Lefkowitz, M.; Shi, V.; Zile, M. R.; Solomon, S. D. Effect of the angiotensin-receptor-neprilysin inhibitor LCZ696 compared with enalapril on mode of death in heart failure patients. *European Heart Journal* **2015,** *36*, (30), 1990-1997.

Chapter 2

1. Simons, F. E.; Simons, K. J. Histamine and H1-antihistamines: celebrating a century of progress. *J. Allergy. Clin. Immunol.* **2011,** *128*, (6), 1139-1150.e4.
2. Simons, F. E. Advances in H1-antihistamines. *N. Engl. J. Med.* **2004,** *351*, (21), 2203-17.
3. Lieberman, P.; Hernandez-Trujillo, V.; Lieberman, J.; Frew, A. J., 89 - Antihistamines. In *Clinical Immunology (Third Edition)*, Rich, R. R.; Fleisher, T. A.; Shearer, W. T.; Schroeder, H. W.; Frew, A. J.; Weyand, C. M., Eds. Mosby: Edinburgh, 2008; pp 1317-1329.
4. Lemke, T. L.; Williams, D. A., *Foye's Principles of Medicinal Chemistry*. Wolters Kluwer Health/Lippincott Williams & Wilkins: 2012.
5. Hilbert, J.; Radwanski, E.; Weglein, R.; Luc, V.; Perentesis, G.; Symchowicz, S.; Zampaglione, N. Pharmacokinetics and dose proportionality of loratadine. *J. Clin. Pharmacol.* **1987,** *27*, (9), 694-8.
6. Ramanathan, R.; Reyderman, L.; Kulmatycki, K.; Su, A. D.; Alvarez, N.; Chowdhury, S. K.; Alton, K. B.; Wirth, M. A.; Clement, R. P.; Statkevich, P.; Patrick, J. E. Disposition of loratadine in healthy volunteers. *Xenobiotica* **2007,** *37*, (7), 753-69.
7. Clark, M. J.; Million, R. P. Allergic rhinitis: market evolution. *Nat. Rev. Drug Discov.* **2009,** *8*, (4), 271-2.
8. Trygstad, T. K.; Hansen, R. A.; Wegner, S. E. Evaluation of product switching after a state Medicaid program began covering loratadine OTC 1 year after market availability. *J. Manag. Care Pharm.* **2006,** *12*, (2), 108-20.
9. Geha, R. S.; Meltzer, E. O. Desloratadine: A new, nonsedating, oral antihistamine. *J. Allergy Clin. Immunol.* **2001,** *107*, (4), 751-62.
10. Molimard, M.; Diquet, B.; Benedetti, M. S. Comparison of pharmacokinetics and metabolism of desloratadine, fexofenadine, levocetirizine and mizolastine in humans.

Fundam. Clin. Pharmacol. **2004,** *18*, (4), 399-411.
11. Ramanathan, R.; Reyderman, L.; Su, A. D.; Alvarez, N.; Chowdhury, S. K.; Alton, K. B.; Wirth, M. A.; Clement, R. P.; Statkevich, P.; Patrick, J. E. Disposition of desloratadine in healthy volunteers. *Xenobiotica* **2007,** *37*, (7), 770-87.
12. Glass, D. J.; Harper, A. S. Assessing satisfaction with desloratadine and fexofenadine in allergy patients who report dissatisfaction with loratadine. *BMC Fam. Pract.* **2003,** *4*, 10.
13. Sun, C. C. Microstructure of Tablet—Pharmaceutical Significance, Assessment, and Engineering. *Pharm. Res.* **2017,** *34*, (5), 918-928.
14. Sun, C. C. Decoding Powder Tabletability: Roles of Particle Adhesion and Plasticity. *J. Adhes. Sci. Technol.* **2011,** *25*, (4-5), 483-499.
15. Ambros, M. C.; Podczeck, F.; Podczeck, H.; Newton, J. M. The characterization of the mechanical strength of chewable tablets. *Pharm. Dev. Technol.* **1998,** *3*, (4), 509-15.
16. Bi, Y.; Sunada, H.; Yonezawa, Y.; Danjo, K.; Otsuka, A.; Iida, K. Preparation and Evaluation of a Compressed Tablet Rapidly Disintegrating in the Oral Cavity. *Chem. Pharm. Bull.* **1996,** *44*, (11), 2121-2127.
17. Krishna, G. R.; Shi, L.; Bag, P. P.; Sun, C. C.; Reddy, C. M. Correlation Among Crystal Structure, Mechanical Behavior, and Tabletability in the Co-Crystals of Vanillin Isomers. *Cryst. Growth Des.* **2015,** *15*, (4), 1827-1832.
18. Wang, C.; Paul, S.; Wang, K.; Hu, S.; Sun, C. C. Relationships among Crystal Structures, Mechanical Properties, and Tableting Performance Probed Using Four Salts of Diphenhydramine. *Cryst. Growth Des.* **2017,** *17*, (11), 6030-6040.
19. Sun, C. C. Materials science tetrahedron--a useful tool for pharmaceutical research and development. *J. Pharm. Sci.* **2009,** *98*, (5), 1671-87.
20. Reutzel-Edens, S. M.; Bush, J. K.; Magee, P. A.; Stephenson, G. A.; Byrn, S. R. Anhydrates and Hydrates of Olanzapine: Crystallization, Solid-State Characterization, and Structural Relationships. *Cryst. Growth Des.* **2003,** *3*, (6), 897-907.
21. Roy, S.; Quiñones, R.; Matzger, A. J. Structural and Physicochemical Aspects of Dasatinib Hydrate and Anhydrate Phases. *Cryst. Growth Des.* **2012,** *12*, (4), 2122-2126.
22. Grzesiak, A. L.; Lang, M.; Kim, K.; Matzger, A. J. Comparison of the four anhydrous polymorphs of carbamazepine and the crystal structure of form I. *J. Pharm. Sci.* **2003,** *92*, (11), 2260-71.
23. Sun, C.; Grant, D. J. Influence of crystal structure on the tableting properties of sulfamerazine polymorphs. *Pharm. Res.* **2001,** *18*, (3), 274-80.
24. Aitipamula, S.; Wong, A. B. H.; Chow, P. S.; Tan, R. B. H. Cocrystallization with flufenamic acid: comparison of physicochemical properties of two pharmaceutical cocrystals. *CrystEngComm* **2014,** *16*, (26), 5793-5801.
25. Liu, L.; Wang, C.; Dun, J.; Chow, A. H. L.; Sun, C. C. Lack of dependence of mechanical properties of baicalein cocrystals on those of the constituent components. *CrystEngComm* **2018,** *20*, (37), 5486-5489.
26. Mannava, M. K. C.; Suresh, K.; Nangia, A. Enhanced Bioavailability in the Oxalate

Salt of the Anti-Tuberculosis Drug Ethionamide. *Crystal Growth & Design* **2016,** *16*, (3), 1591-1598.
27. Suresh, K.; Nangia, A. Lornoxicam Salts: Crystal Structures, Conformations, and Solubility. *Crystal Growth & Design* **2014,** *14*, (6), 2945-2953.
28. Fell, J. T.; Newton, J. M. Determination of tablet strength by the diametral-compression test. *J. Pharm. Sci.* **1970,** *59*, (5), 688-91.
29. Joiris, E.; Martino, P. D.; Berneron, C.; Guyot-Hermann, A.-M.; Guyot, J.-C. Compression Behavior of Orthorhombic Paracetamol. *Pharm. Res.* **1998,** *15*, (7), 1122-1130.
30. Heckel, R. W. An analysis of powder compaction phenomena. *Trans. Metall. Soc. AIME* **1961,** *221*, 1001-1008.
31. Heckel, R. W. Density-Pressure Relationships in Powder Compaction. *Trans. Metall. Soc. AIME* **1961,** *221*, 671-675.
32. Kuentz, M.; Leuenberger, H. Pressure susceptibility of polymer tablets as a critical property: a modified Heckel equation. *J Pharm Sci* **1999,** *88*, (2), 174-9.
33. Owens, D. K.; Wendt, R. C. Estimation of the surface free energy of polymers. *J. Appl. Polym.* **1969,** *13*, (8), 1741-1747.
34. Bryant, M. J.; Maloney, A. G. P.; Sykes, R. A. Predicting mechanical properties of crystalline materials through topological analysis. *CrystEngComm* **2018,** *20*, (19), 2698-2704.
35. M. J. Turner, J. J. M., S. K. Wolff, D. J. Grimwood, P. R. Spackman, D. Jayatilaka and M. A. Spackman *CrystalExplorer17*, University of Western Australia: 2017.
36. Turner, M. J.; Grabowsky, S.; Jayatilaka, D.; Spackman, M. A. Accurate and Efficient Model Energies for Exploring Intermolecular Interactions in Molecular Crystals. *J. Phys. Chem. Lett.* **2014,** *5*, (24), 4249-55.
37. Turner, M. J.; Thomas, S. P.; Shi, M. W.; Jayatilaka, D.; Spackman, M. A. Energy frameworks: insights into interaction anisotropy and the mechanical properties of molecular crystals. *Chem. Commun. (Camb)* **2015,** *51*, (18), 3735-8.
38. Bhatt, P. M.; Desiraju, G. R. Form I of desloratadine, a tricyclic antihistamine. *Acta Crystallogr. C* **2006,** *62*, (6), o362-o363.
39. Popovic, G.; Cakar, M.; Agbaba, D. Acid-base equilibria and solubility of loratadine and desloratadine in water and micellar media. *J. Pharm. Biomed. Anal.* **2009,** *49*, (1), 42-7.
40. Sun, C. C. A material-sparing method for simultaneous determination of true density and powder compaction properties--aspartame as an example. *Int. J. Pharm.* **2006,** *326*, (1-2), 94-9.
41. Osei-Yeboah, F.; Chang, S. Y.; Sun, C. C. A critical Examination of the Phenomenon of Bonding Area - Bonding Strength Interplay in Powder Tableting. *Pharm. Res.* **2016,** *33*, (5), 1126-32.
42. Wang, C.; Sun, C. C. Identifying Slip Planes in Organic Polymorphs by Combined Energy Framework Calculations and Topology Analysis. *Cryst. Growth Des.* **2018,** *18*, (3),

1909-1916.
43. Singaraju, A. B.; Nguyen, K.; Gawedzki, P.; Herald, F.; Meyer, G.; Wentworth, D.; Swenson, D. C.; Stevens, L. L. Combining Crystal Structure and Interaction Topology for Interpreting Functional Molecular Solids: A Study of Theophylline Cocrystals. *Cryst. Growth Des.* **2017,** *17*, (12), 6741-6751.
44. Joshi, T. V.; Singaraju, A. B.; Shah, H. S.; Morris, K. R.; Stevens, L. L.; Haware, R. V. Structure–Mechanics and Compressibility Profile Study of Flufenamic Acid:Nicotinamide Cocrystal. *Cryst. Growth Des.* **2018,** *18*, (10), 5853-5865.
45. Edwards, A. J.; Mackenzie, C. F.; Spackman, P. R.; Jayatilaka, D.; Spackman, M. A. Intermolecular interactions in molecular crystals: what's in a name? *Faraday Discuss.* **2017,** *203*, (0), 93-112.
46. Wang, C.; Sun, C. C. Computational Techniques for Predicting Mechanical Properties of Organic Crystals: A Systematic Evaluation. *Mol Pharm* **2019,** *16*, (4), 1732-1741.
47. Fichtner, F.; Mahlin, D.; Welch, K.; Gaisford, S.; Alderborn, G. Effect of surface energy on powder compactibility. *Pharm. Res.* **2008,** *25*, (12), 2750-9.
48. Sun, C. C., Role of Surface Free Energy in Powder Behavior and Tablet Strength. In *Adhesion Science: Applications to Pharmaceutical, Medical and Dental Fields*, Mittal, K.; Etzler, F., Eds. Scrivener Publishing /John Wiley & Sons: 2017; pp 75-88.
49. Hiestand, E. N. Dispersion forces and plastic deformation in tablet bond. *J. Pharm. Sci.* **1985,** *74*, (7), 768-70.
50. Steiner, T.; R. Desiraju, G. Distinction between the weak hydrogen bond and the van der Waals interaction. *Chem. Commun.* **1998**, (8), 891-892.
51. Luangtana-Anan, M.; Fell, J. T. Bonding mechanisms in tabletting. *Int. J. Pharm.* **1990,** *60*, (3), 197-202.
52. Aakeröy, C. B.; Seddon, K. R. The hydrogen bond and crystal engineering. *Chem. Soc. Rev.* **1993,** *22*, (6), 397-407.
53. Desiraju, G. R. Crystal engineering: from molecule to crystal. *J. Am. Chem. Soc.* **2013,** *135*, (27), 9952-67.
54. Vishweshwar, P.; McMahon, J. A.; Bis, J. A.; Zaworotko, M. J. Pharmaceutical co-crystals. *J Pharm Sci* **2006,** *95*, (3), 499-516.

Chapter 3

1. Simons, F. E. R. Advances in H1-Antihistamines. *N Engl J Med.* **2004,** *351*, (21), 2203-2217.
2. Haria, M.; Fitton, A.; Peters, D. H. Loratadine. A reappraisal of its pharmacological properties and therapeutic use in allergic disorders. *Drugs* **1994,** *48*, (4), 617-637.
3. Khan, M. Z.; Rausl, D.; Zanoski, R.; Zidar, S.; Mikulcic, J. H.; Krizmanic, L.; Eskinja, M.; Mildner, B.; Knezevic, Z. Classification of loratadine based on the biopharmaceutics

drug classification concept and possible in vitro-in vivo correlation. *Biol Pharm Bull* **2004,** *27*, (10), 1630-5.
4. Hilbert, J.; Radwanski, E.; Weglein, R.; Luc, V.; Perentesis, G.; Symchowicz, S.; Zampaglione, N. Pharmacokinetics and dose proportionality of loratadine. *J Clin Pharmacol* **1987,** *27*, (9), 694-8.
5. Sora, D. I.; Udrescu, S.; David, V.; Medvedovici, A. Validated ion pair liquid chromatography/fluorescence detection method for assessing the variability of the loratadine metabolism occurring in bioequivalence studies. *Biomed Chromatogr.* **2007,** *21*, (10), 1023-1029.
6. Omar, L.; El-Barghouthi, M. I.; Masoud, N. A.; Abdoh, A. A.; Al Omari, M. M.; Zughul, M. B.; Badwan, A. A. Inclusion Complexation of Loratadine with Natural and Modified Cyclodextrins: Phase Solubility and Thermodynamic Studies. *J Solution Chem.* **2007,** *36*, (5), 605-616.
7. Patil, P.; Paradkar, A. Porous polystyrene beads as carriers for self-emulsifying system containing loratadine. *AAPS PharmSciTech* **2006,** *7*, (1), E199-E205.
8. Frizon, F.; Eloy, J. d. O.; Donaduzzi, C. M.; Mitsui, M. L.; Marchetti, J. M. Dissolution rate enhancement of loratadine in polyvinylpyrrolidone K-30 solid dispersions by solvent methods. *Powder Technol.* **2013,** *235*, 532-539.
9. Chang, R.; Fu, Q.; Yu, P.; Wang, L.; Li, Y.; Du, W.; Chang, C.; Zeng, A. A new polymorphic form and polymorphic transformation of loratadine. *RSC Adv.* **2016,** *6*, (88), 85063-85073.
10. Wang, J.; Chang, R.; Zhao, Y.; Zhang, J.; Zhang, T.; Fu, Q.; Chang, C.; Zeng, A. Coamorphous Loratadine-Citric Acid System with Enhanced Physical Stability and Bioavailability. *AAPS PharmSciTech* **2017,** *18*, (7), 2541-2550.
11. Schiffman, S. S. Influence of medications on taste and smell. *World J Otorhinolaryngol Head Neck Surg* **2018,** *4*, (1), 84-91.
12. Desiraju, G. R., *Crystal Engineering: The Design of Organic Solids*. Elsevier: 1989.
13. Steed, J. W. The role of co-crystals in pharmaceutical design. *Trends Pharmacol. Sci.* **2013,** *34*, (3), 185-193.
14. Blagden, N.; de Matas, M.; Gavan, P. T.; York, P. Crystal engineering of active pharmaceutical ingredients to improve solubility and dissolution rates. *Adv. Drug Deliv. Rev.* **2007,** *59*, (7), 617-30.
15. Schultheiss, N.; Newman, A. Pharmaceutical Cocrystals and Their Physicochemical Properties. *Cryst Growth Des* **2009,** *9*, (6), 2950-2967.
16. Duggirala, N. K.; Perry, M. L.; Almarsson, O.; Zaworotko, M. J. Pharmaceutical cocrystals: along the path to improved medicines. *Chem Commun (Camb)* **2016,** *52*, (4), 640-55.
17. Serajuddin, A. T. M. Salt formation to improve drug solubility. *Adv. Drug Deliv. Rev.* **2007,** *59*, (7), 603-616.
18. Berge, S. M.; Bighley, L. D.; Monkhouse, D. C. Pharmaceutical Salts. *J Pharm Sci.* **1977,** *66*, (1), 1-19.

19. Groom, C. R.; Allen, F. H. The Cambridge Structural Database in retrospect and prospect. *Angew Chem Int Ed Engl* **2014,** *53*, (3), 662-71.
20. El-Gazayerly, O. N.; Rakkanka, V.; Ayres, J. W. Novel Chewable Sustained-Release Tablet Containing Verapamil Hydrochloride. *Pharm. Dev. Technol.* **2004,** *9*, (2), 181-188.
21. Suzuki, H.; Onishi, H.; Hisamatsu, S.; Masuda, K.; Takahashi, Y.; Iwata, M.; Machida, Y. Acetaminophen-containing chewable tablets with suppressed bitterness and improved oral feeling. *Int. J. Pharm.* **2004,** *278*, (1), 51-61.
22. Banerjee, R.; Bhatt, P. M.; Ravindra, N. V.; Desiraju, G. R. Saccharin Salts of Active Pharmaceutical Ingredients, Their Crystal Structures, and Increased Water Solubilities. *Cryst Growth Des* **2005,** *5*, (6), 2299-2309.
23. Wang, C.; Hu, S.; Sun, C. C. Expedited Development of Diphenhydramine Orally Disintegrating Tablet through Integrated Crystal and Particle Engineering. *Mol. Pharm.* **2017,** *14*, (10), 3399-3408.
24. Popovic, G.; Cakar, M.; Agbaba, D. Acid-base equilibria and solubility of loratadine and desloratadine in water and micellar media. *J Pharm Biomed Anal* **2009,** *49*, (1), 42-7.
25. Hübschle, C. B.; Sheldrick, G. M.; Dittrich, B. ShelXle: a Qt graphical user interface for SHELXL. *J. Appl. Crystallogr.* **2011,** *44*, (Pt 6), 1281-1284.
26. Wang, C.; Perumalla, S. R.; Lu, R.; Fang, J.; Sun, C. C. Sweet Berberine. *Cryst. Growth Des.* **2016,** *16*, (2), 933-939.
27. Fell, J. T.; Newton, J. M. Determination of Tablet Strength by the Diametral-Compression Test. *J Pharm Sci.* **1970,** *59*, (5), 688-691.
28. Gupta, A.; Chidambaram, N.; Khan, M. A. An index for evaluating difficulty of Chewing Index for chewable tablets *Drug Dev. Ind. Pharm.* **2015,** *41*, (2), 239-243.
29. Sun, C. C. Quantifying effects of moisture content on flow properties of microcrystalline cellulose using a ring shear tester. *Powder Technol.* **2016,** *289*, 104-108.
30. Osei-Yeboah, F.; Sun, C. C. Validation and applications of an expedited tablet friability method. *Int J Pharm.* **2015,** *484*, (1), 146-155.
31. Aitipamula, S.; Banerjee, R.; Bansal, A. K.; Biradha, K.; Cheney, M. L.; Choudhury, A. R.; Desiraju, G. R.; Dikundwar, A. G.; Dubey, R.; Duggirala, N.; Ghogale, P. P.; Ghosh, S.; Goswami, P. K.; Goud, N. R.; Jetti, R. R. K. R.; Karpinski, P.; Kaushik, P.; Kumar, D.; Kumar, V.; Moulton, B.; Mukherjee, A.; Mukherjee, G.; Myerson, A. S.; Puri, V.; Ramanan, A.; Rajamannar, T.; Reddy, C. M.; Rodriguez-Hornedo, N.; Rogers, R. D.; Row, T. N. G.; Sanphui, P.; Shan, N.; Shete, G.; Singh, A.; Sun, C. C.; Swift, J. A.; Thaimattam, R.; Thakur, T. S.; Kumar Thaper, R.; Thomas, S. P.; Tothadi, S.; Vangala, V. R.; Variankaval, N.; Vishweshwar, P.; Weyna, D. R.; Zaworotko, M. J. Polymorphs, Salts, and Cocrystals: What's in a Name? *Cryst. Growth Des.* **2012,** *12*, (5), 2147-2152.
32. Grothe, E.; Meekes, H.; Vlieg, E.; ter Horst, J. H.; de Gelder, R. Solvates, Salts, and Cocrystals: A Proposal for a Feasible Classification System. *Cryst. Growth Des.* **2016,** *16*, (6), 3237-3243.
33. Kong, M.; Fu, X.; Li, J.; Li, J.; Chen, M.; Deng, Z.; Zhang, H. Sweet pharmaceutical salts of stanozolol with enhanced solubility and physical stability. *CrystEngComm* **2016,**

18, (45), 8739-8746.
34. Perumalla, S. R.; Pedireddi, V. R.; Sun, C. C. Design, Synthesis, and Characterization of New 5-Fluorocytosine Salts. *Mol. Pharm.* **2013,** *10*, (6), 2462-2466.
35. Muster, T. H.; Prestidge, C. A.; Hayes, R. A. Water adsorption kinetics and contact angles of silica particles. *Colloids Surf. A* **2001,** *176*, (2), 253-266.
36. Puri, V.; Dantuluri, A. K.; Kumar, M.; Karar, N.; Bansal, A. K. Wettability and surface chemistry of crystalline and amorphous forms of a poorly water soluble drug. *Eur. J. Pharm. Sci.* **2010,** *40*, (2), 84-93.
37. Guzman, H. R.; Tawa, M.; Zhang, Z.; Ratanabanangkoon, P.; Shaw, P.; Gardner, C. R.; Chen, H.; Moreau, J. P.; Almarsson, O.; Remenar, J. F. Combined use of crystalline salt forms and precipitation inhibitors to improve oral absorption of celecoxib from solid oral formulations. *J. Pharm. Sci.* **2007,** *96*, (10), 2686-702.
38. Samie, A.; Desiraju, G. R.; Banik, M. Salts and Cocrystals of the Antidiabetic Drugs Gliclazide, Tolbutamide, and Glipizide: Solubility Enhancements through Drug–Coformer Interactions. *Cryst. Growth Des.* **2017,** *17*, (5), 2406-2417.
39. Sanphui, P.; Goud, N. R.; Khandavilli, U. B. R.; Nangia, A. Fast Dissolving Curcumin Cocrystals. *Cryst. Growth Des.* **2011,** *11*, (9), 4135-4145.
40. Almansa, C.; Mercè, R.; Tesson, N.; Farran, J.; Tomàs, J.; Plata-Salamán, C. R. Co-crystal of Tramadol Hydrochloride–Celecoxib (ctc): A Novel API–API Co-crystal for the Treatment of Pain. *Cryst. Growth Des.* **2017,** *17*, (4), 1884-1892.
41. Liu, F.; Song, Y.; Liu, Y.-N.; Li, Y.-T.; Wu, Z.-Y.; Yan, C.-W. Drug-Bridge-Drug Ternary Cocrystallization Strategy for Antituberculosis Drugs Combination. *Cryst. Growth Des.* **2018,** *18*, (3), 1283-1286.
42. FDA-CDER, Quality Attribute Considerations for Chewable Tablets Guidance for Industry. 2018.
43. Ohrem, H. L.; Schornick, E.; Kalivoda, A.; Ognibene, R. Why is mannitol becoming more and more popular as a pharmaceutical excipient in solid dosage forms? *Pharm. Dev. Technol.* **2014,** *19*, (3), 257-262.
44. Paul, S.; Chang, S.-Y.; Dun, J.; Sun, W.-J.; Wang, K.; Tajarobi, P.; Boissier, C.; Sun, C. C. Comparative analyses of flow and compaction properties of diverse mannitol and lactose grades. *Int. J. Pharm.* **2018,** *546*, (1), 39-49.
45. Paul, S.; Tajarobi, P.; Boissier, C.; Sun, C. C. Tableting performance of various mannitol and lactose grades assessed by compaction simulation and chemometrical analysis. *Int. J. Pharm.* **2019,** *566*, 24-31.
46. Kimura, S.-i.; Uchida, S.; Kanada, K.; Namiki, N. Effect of granule properties on rough mouth feel and palatability of orally disintegrating tablets. *Int. J. Pharm.* **2015,** *484*, (1), 156-162.
47. Rowe, R.; Sheskey, P.; Quinn, M.; Association, A. P.; Press, P.; Others, *Handbook of pharmaceutical excipients*. Pharmaceutical press London: 2009; Vol. 6.
48. Sun, C. C. Setting the bar for powder flow properties in successful high speed tableting. *Powder Technol.* **2010,** *201*, (1), 106-108.

49. Joiris, E.; Martino, P. D.; Berneron, C.; Guyot-Hermann, A.-M.; Guyot, J.-C. Compression Behavior of Orthorhombic Paracetamol. *Pharm. Res.* **1998,** *15*, (7), 1122-1130.
50. Sun, C.; Grant, D. J. W. Influence of Crystal Structure on the Tableting Properties of Sulfamerazine Polymorphs. *Pharm Res.* **2001,** *18*, (3), 274-280.
51. Shafer, E. G. E.; Wollish, E. G.; Engel, C. E. The "Roche" Friabilator. *J. Am. Pharm. Assoc. Am. Pharm. Assoc.* **1956,** *45*, (2), 114-116.
52. Soh, J. L.; Grachet, M.; Whitlock, M.; Lukas, T. Characterization, optimisation and process robustness of a co-processed mannitol for the development of orally disintegrating tablets. *Pharm. Dev. Technol.* **2013,** *18*, (1), 172-85.
53. Paul, S.; Sun, C. C. Dependence of Friability on Tablet Mechanical Properties and a Predictive Approach for Binary Mixtures. *Pharm. Res.* **2017,** *34*, (12), 2901-2909.